prepared for *JPC A* for the new section on New Tools and Methods in Experiment and Theory
revised on Jan. 31, 2019

Revised M11 Exchange–Correlation Functional for Electronic Excitation Energies and Ground–State Properties

Pragya Verma,[1,*] Ying Wang,[2,3] Soumen Ghosh,[1] Xiao He,[2,4,*] and Donald G. Truhlar[1,*]

[1]*Department of Chemistry, Chemical Theory Center, Nanoporous Materials Genome Center, and Minnesota Supercomputing Institute, University of Minnesota, Minneapolis, Minnesota, 55455-0431, USA*
[2]*Shanghai Engineering Research Center of Molecular Therapeutics and New Drug Development, School of Chemistry and Molecular Engineering, East China Normal University, Shanghai, 200062, China*
[3]*The National and Local Joint Engineering Laboratory of Animal Peptide Drug Development, College of Life Sciences, Hunan Normal University, Changsha, 410006, China*
[4]*NYU-ECNU Center for Computational Chemistry at NYU Shanghai, Shanghai, 200062, China*

*E-mail: verma045@umn.edu (P.V.), xiaohe@phy.ecnu.edu.cn (X.H.), and truhlar@umn.edu (D.G.T.)

Abstract. The ability of Kohn-Sham density functional theory (KS-DFT) to accurately predict various types of electronic excitation energies with (necessarily approximate) exchange-correlation functionals faces several challenges. Chief among these is that valence excitations are usually inherently multiconfigurational and therefore best treated by functionals with local exchange, whereas Rydberg and charge transfer excitations are often better treated with nonlocal exchange. The question arises of whether one can optimize a functional such that all three kinds of excitations (valence, Rydberg, and charge transfer – including long-range charge transfer) are treated in a balanced and accurate way. The goal of the present work is to try to answer that question and then to optimize a functional with the best possible balanced behavior. Of the variety of functional types available, we select range-separated hybrid meta functionals because (i) range separation allows the percentage of Hartree–Fock (HF) exchange to change with interelectronic separation, and therefore, one can have 100% HF exchange at large interelectronic separations, which gives good performance for long-range charge-transfer excitations, while the range separation allows one to simultaneously have smaller values of HF exchange at small and intermediate inter-electronic separations, which give good performance for valence and Rydberg excitations and (ii) meta functionals allow one to obtain better accuracy with high HF exchange than is possible with functionals whose local part depends only on spin densities and their gradients. This work starts with the range-separated hybrid meta functional, M11, and re-optimizes it (with stronger smoothness restraints) against electronic excitation energies and ground-state properties to obtain a new functional called revM11 that gives good performance for all three types of electronic excitations and at the same time gives very good predictions across-the-board for ground-state properties.

1. Introduction

Kohn-Sham density functional theory (DFT)[1] was originally proposed using local exchange-correlation functionals, but later on hybrid functionals including some percentage of nonlocal Hartree-Fock (HF) exchange were found to have several advantages.[2] The first successful functionals combining a portion of HF exchange with local DFT were proposed by Becke in 1993.[3,4] Very soon hybrid functionals became widely used in chemistry, and the improvement in accuracy is especially pronounced for barrier heights, excitation energies, and charge transfer.[5] Becke originally justified the admixture of HF exchange and local exchange by the adiabatic connection, and later it was justified more fundamentally as the generalized Kohn-Sham scheme.[6]

There is more than one way to mix HF exchange with local DFT. The original approach involved substituting a percentage of local exchange by the same percentage of HF exchange, with the percentage (which we label as X) independent of interelectronic separation; this yields what is called a global hybrid functional. More generally the percentage can vary with interelectronic separation, and functionals with this feature are called range separated or local hybrids. Five kinds of functionals fall in this category: (i) long-range corrected functionals for which the percentage of HF exchange increases monotonically with interelectronic separation up to 100%, (ii) Coulomb-attenuated functionals in which the percentage of HF exchange increases monotonically with interelectronic separation but not all the way up to 100%, (iii) screened hybrid functionals for which the percentage of HF exchange decreases monotonically with interelectronic separation and goes down to 0%, (iv) multi-range hybrid functionals in which the percentage of HF exchange is a nonmonotonic function of interelectronic separation, and (v) local hybrid functionals for which HF exchange changes with interelectronic separation in a way defined by a local mixing function. (References for types i–iv are given in Section 5, and a review of functionals of type v is available.[7]) Long-range-corrected functionals are particularly well suited to our present goal because some properties – most importantly long-range charge transfer excitations – are only predicted even qualitatively correctly with functionals having 100% HF exchange at long range. However, functionals with 100% HF exchange at long range often show deterioration of accuracy for other kinds of electronic transitions. This is part of a general difficulty of achieving across-the-board good performance for excitation energies because improving a functional for one type of excitation can worsen it for other types. For example, high HF exchange usually improves long-range charge-transfer excitations but at the same time it can worsen short-range charge-transfer excitations by overestimating it and can worsen valence excitation energies by increasing static

correlation error, which is more important for valence states because they are usually inherently multiconfigurational.

The primary goal of the work reported here is the design of a long-range corrected hybrid density functional with the objective of obtaining reasonably good performance for all three types of electronic excitations – valence, Rydberg, and charge transfer – and within charge transfer for both short-range and long-range charge-transfer excitations. Furthermore, within the latitude allowed by satisfying this primary objective, we want the functional to be as good as possible for as many ground-state properties as possible.

The long-range corrected density functional M11[8] has 42.8% HF exchange at short interelectronic separation and 100% HF exchange at long interelectronic separation (i.e., X increases from 42.8 to 100 as the interelectronic distance increases), and the range separation parameter, ω, which gives the rate at which HF exchange increases with distance (it is defined more precisely below) has a value of 0.25 a_0^{-1}, where a_0 denotes a bohr (1 a_0 = 0.529177 Å). The M11 functional form with these parameters for HF exchange has been successfully used for treating electronic excitation energies of both organic and inorganic molecules and ground-state properties; however, it has larger than desirable errors in certain cases, in particular, for long-range charge-transfer excitations where the overlap of density between the orbitals participating in the excitation is negligible or zero. Because the M11 functional has already been shown to be good for most of the excitation types, we use it as a starting point to obtain a balanced treatment for all types of excitation energies. We revise the M11 functional by optimizing X and ω along with other parameters of the M11 functional form to obtain improved ground-state properties and excitation energies of molecules – this revised functional is called revM11. We optimize revM11 for molecules, but not for solids. We do not attempt to optimize revM11 for solids because calculations with long-range corrected functionals are very expensive in plane wave codes, and therefore, this kind of functional form is not a favored choice for calculations on solids.

The curation of databases is a central component in our method for optimization and testing of density functionals. We put diverse data in the databases to facilitate the broad testing of new and existing functionals. One example of diversity is that the database should contain both weakly correlated species, which are molecules or transition states for which a single configuration state function makes a good zero-order reference wave function, and strongly correlated species, which are molecules or transition states that are only well described, even in zero-order, by using two or

more configuration state functions. These two classes of species will be respectively called single-reference (SR) species and multireference (MR) species; MR species are also called inherently multiconfigurational.

In the present work, not only do we optimize the new revM11 functional, but also, we compare its performance to the performance of various popular local, global hybrid, and range-separated hybrid density functionals on databases with SR and MR species, with ground-state and excited-state molecular properties, and with energetic and geometric properties of molecules.

This article is organized as follows. Section 2 presents the training and test databases used in this work. Section 3 gives the basis sets used for all the databases. Section 4 gives the computational details. Section 5 gives the functionals tested for comparison. Section 6 presents the revM11 functional form. Section 7 presents the optimization scheme for the revM11 functional. Section 8 gives the newly optimized parameters. Section 9 presents the performance of the revM11 functional and other density functionals tested in this work. In Section 10 we attempt a comprehensive ranking, in Section 11 we discuss other possible strategies for optimizing density functionals, and Section 12 gives concluding remarks.

2. Databases

Our databases of reference values of chemical properties are composed of a combination experimental data and – especially where accurate experimental data is not available – of benchmark-quality theoretical data. The quality of a database is limited by the accuracy of this data. We and other coworkers have developed several databases and updating the reference values with more accurate values has been an ongoing process.

Our databases have been organized into many subdatabases[5,9,10,11,12,13,14,15,16,17,18] (the subdatabases are referred to as both databases and subdatabases, depending on the context). In the present work, we use subdatabases that were used in our recent work (Database 2018[18]) plus additional subdatabases that mainly have excitation energy (EE) data. This updated compilation is referred to as Database 2019. Table 1 lists the databases that we have used in our recent past work and the references[5,14,15,16,17,18,19] where they were presented; the last line of the table refers to the database used in the present work, which is called Database 2019, developed as part of the present work.

Database 2019 has two main components: training set and additional test data; the former has 31 subdatabases and the latter has 25 subdatabases. Both the training and additional test data are divided into ground-state properties and excitation energies.

Table 1. Databases used in some of our recent and present work.

Name	Description[a]	Reference[b]
Common Database 2.0	CE345 + PE39 + CS20 + PS47	review [5]
Database 2015	Reorganized old and new data	GAM[14]
Database 2017	Database 2015 + more data	revM06-L[17]
Database 2018	Database 2017 + nine databases from Ref. 19	revM06[18]
Database 2019	Database 2018 + more data	present work

[a]The subdatabases are explained in the references.

[b]This column provides references for the paper in which the entire database was first reported. The interested reader should see these papers and older papers cited therein for more complete explanations.

2.1 Database 2019 – data used for training as well as testing

The 31 subdatabases of Database 2019 that are used for training the new functional are given in Table 2. These subdatabases comprise data only of molecules and ions, and they include energetic data, and geometric data for ground states and also excitation energies. Some of the ground-state properties databases are labeled as SR or MR depending on diagnostic tests performed with the B_1 diagnostic.[20] Some of the ground state properties are labeled BE or AE depending on whether we calculate bond energy or atomization energy. The bond energies involve breaking of specific bonds, while atomization energies involve breaking of all the bonds. For the AE databases, the atomization energy of each molecule is divided by the number of bonds, so the error actually refers to the average bond energy; for this purpose, double and triple bonds are counted as one bond.

Three of the excited-state databases (3dEE8, 4dAEE5, and pAEE5) involve excitation energies calculated using the ΔSCF method; the other two (EE23 and LRCTEE9) involve time-dependent DFT with linear-response approximation.

We added Fe_2 dimer to 3dAEE7 database in a previous work,[15] and the combined database is called 3dEE8. Seven of the excitations in the 3dEE8 database involve a change in spin multiplicity, but one datum – that for the Ca^+ ion – does not involve a change in spin multiplicity but rather involves 3s $\rightarrow$ 3d excitation.

Table 2. Subset of Database 2019 used for both training and testing

Database[a]	Description	Inverse weight[b]	Reference[c]
Ground-state energies			
SR-MGM-BE8	Single-reference main-group metal bond energies	12.0	14,21,22
SR-MGN-BE107	Single-reference main-group non-metal bond energies	0.04	14,23
SR-TM-BE15	Single-reference transition-metal bond energies	0.45	14,22,24,25
MR-MGM-BE4	Multi-reference main-group metal bond energies	0.40	14,21
MR-MGN-BE17	Multi-reference main-group non-metal bond energies	0.80	14
MR-TM-BE12	Multi-reference transition-metal bond energies	4.40	14,22,25
MR-TMD-BE3	Multi-reference transition-metal dimer bond energies	1.30	14,26
HTBH38/18	Hydrogen transfer barrier heights (38 data)	0.10	5,27,28
NHTBH38/18	Non-hydrogen transfer barrier heights (38 data)	0.10	5,14,27,28
NCCE30/18	Noncovalent complexation energies (30 data)	0.048	5,11,12, 14,29,30,31,32
NGD21/18	Noble gas dimer weak interactions (21 data)	0.01	5,14,33
S6x6	Subset of S66x8 – described in Table 3 (36 data)	0.02	34
IP23	Ionization potentials	0.40	35,36
EA13/03	Electron affinities (13 data)	0.12	5
PA8	Proton affinities	0.20	5,37
2pIsoE4	Isomerization energies involving atoms of the 2p block	12.0	38
4pIsoE4	4p isomerization energies	12.0	38
IsoL6/11	Isomerization energies of large molecules (6 data)	0.40	39
πTC13	Thermochemistry of π systems	12.0	37,40,41
AE17	Atomic energies	12.0	42
HC7/11	Hydrocarbon chemistry (7 data)	0.23	43
SMAE3/19[d]	Sulfur molecules atomization energies (3 data)	1.00	44,45,46
DC9/19[e]	Difficult cases (9 data)	1.00	47
ABDE13	Alkyl bond dissociation energies	12.0	16
Ground-state bond lengths			
DGL6	Bond lengths for diatoms with light atoms	0.01	5,14
DGH4	Bond lengths for diatoms with one or more nonhydrogenic atom	0.01	48,49
Excitation energies calculated by ΔSCF			
3dEE8	Excitation energies of 3d transition-metal atoms and Fe_2	0.30	21,26,36
4dAEE5	4d transition-metal atomic excitation energies	5.00	50
pAEE5	p-block atomic excitation energies	12.0	51
Excitation energies calculated by LR-TDDFT			
EE23[f]	Excitation energies of molecules	NA[g]	11,52,53,54,55,56
LRCTEE9	Excitation energies of long-range charge transfer complexes	NA[g]	57

[a] When not stated otherwise, the number of data is given by the number ending the database name.

[b] Inverse weight is the reciprocal of the weight used with each database in the training function F defined by equation 3 in Section 7. Its unit is kcal/mol for databases with energies and Å for databases with geometries.

[c] References for reference data, which means geometries and reference values.

[d] For the SMAE3/19 database, the error for each of the three molecules has been divided by the number of bonds. Division of the error by the number of bonds was not done in our previous work that presented the SMAE3 database.

[e]For the $P_4O_{10} \rightarrow P_4 + 5O_2$ reaction in the DC9 database, the error was divided by the net number of bonds being broken (equals 5), which is defined as the difference between the number of bonds being made and the number of bonds being broken. Therefore, in this work we renamed DC9/18 to DC9/19.

[f]Furan and hexatriene geometries are from Ref. 54. Water geometry is from Ref. 11. B-TCNE geometry is from Ref. 53. Geometries of the other 14 of the 18 molecules in the EE23 database are from Ref. 56.

[g]NA = Not applicable

2.2 Database 2019 – additional test data

The 25 subdatabases of Database 2019 that are used for further testing of the new density functional and for comparison to results obtained with other density functionals are given in Table 3. The ground-state properties included in these tests are bond energies, ionization potentials, barrier heights, self-interaction error, noncovalent interactions energies and potential energy curves, bond lengths, dipole moments, and delocalization error. The excitation energies include valence excitations, Rydberg excitations, and intramolecular and intermolecular charge-transfer excitations. We include appreciable diversity in the excited-state databases by considering both atoms and molecules, by considering both organic and inorganic molecules, by considering both vertical and adiabatic valence excitations, and by considering both short-range and long-range intermolecular charge-transfer excitations.

Table 3. Additional test data in Database 2019

Database[a]	Description	Ref.[b]
Ground-state energies		
Al2X6	Dimerization energies of aluminum compounds	19
BHDIV10	Barrier heights of diverse reactions	19
BHPERI26	Barrier heights of pericyclic reactions	19
BHROT27	Barrier heights for rotation around single bonds	19
DIPCS10	Double-ionization potentials of closed-shell systems	19
HeavySB11	Dissociation energies in heavy-element compounds	19
PX13	Proton-exchange barriers in H_2O, NH_3, HF clusters	19
SIE4x4	Self-interaction-error (16 data)	19
YBDE18	Ylide bond-dissociation energy	19,58
S492	Subset of S66x8 for noncovalent interaction energies by removing S6x6[c]	34
TMBH22	Transition-metal reaction barrier heights of Mo, W, Zr, and Re reactions	59,60,61
WCCR10	Ligand dissociation energies of large cationic transition-metal complexes	62,63
ASNC2	Atmospheric sulfur-nitrogen cluster binding energies	64
Ground-state dipole moments		
DM79	Dipole moments	65,66,NIST
Ground-state noncovalent potential energy curves		

PEC4	Potential energy curves of Ar_2, Kr_2, KrHe, Ne_2 (4 curves)	67
Ground-state bond lengths		
TSG48	Transition state geometries (16 transition structures with 3 distances for each)	68
MGBL193[d]	Bond lengths of main-group compounds	69
TMDBL10	Transition-metal dimer bond lengths	70
Test of ground-state delocalization error		
NaCl	Charge on Na in NaCl at 10 Å interatomic separation (1 datum)	NA[e]
Excitation energies calculated by LR-TDDFT		
EEA11	Excitation energies of atoms	71
AEE15	Adiabatic excitation energies of molecules	72
EEAroT5	Excitation energies of aromatic molecule complexes with TCNE	53
EE69	Excitation energies of organic molecules (30 valence + 39 Rydberg states)	73
EER5	Excitation energies of retinal and dihydroretinal	74,75
LRCTEE2	Excitation energies of long-range charge transfer complexes	57

[a] When not stated otherwise, the number of data is given by the number ending the database name.

[b] References for reference data, which means geometries and reference values.

[c] The S66x8 database consists of interaction energies that are especially relevant to biomolecular structures. The S66x8 has 528 data, and we divided it in various ways: Division 1 is into the S6x6 subset, which is in Table 2 (used for training), and the remaining 492 data, called S492. The second division is into S66, which contains 66 data at equilibrium internuclear separations of the complexes and S462, which contains the data at nonequilibrium geometries; S66 is then divided into DD23, HB23, and Mix20. The third division is into S6x6, S66, and data remaining after data in those subdatabases are removed; because six data occur in both S66 and S6x6, the remaining number of data is 432, and the database containing these data is called S432.

[d] The SE47 database was presented in Ref. 16; it has 193 bond lengths of 47 semi-experimental (SE) equilibrium structures taken from Ref. 69, and it is here renamed as MGBL193 to conform to our conventions for naming subdatabases.

[e] NA = Not applicable

3. Basis sets

The basis sets used with each database are given in Table 4. To evaluate the performance of density functionals on a given database, the same basis set is used with all the functionals. Most of the basis sets of Table 4 are the same as those used in our previous work,[14,15,16,17,18] but for some of them, changes were made, and the complete updated list is provided in Table 4.

Table 4. The basis sets used and the type of calculation performed (optimization versus single-point calculation) on each database.

Database	Type[a]	System or subdatabase[b]	Basis set(s)[c]
Database 2019 – ground-state properties used for training			
SR-MGM-BE8	SP	AlCl, $AlCl_3$, AlF_3, ZnSe, ZnCl	def2-QZVP[76];
		KOH	Feller's CVQZ (K), jun-cc-pV(Q+d)Z[77,78,79] (O), aug-cc-pVQZ (H);
		NaO	cc-pCVQZ (Na), jun-cc-pV(Q+d)Z (O);
		LiCl	cc-pCVQZ (Li), jun-cc-pV(Q+d)Z (Cl)
SR-MGN-BE107	SP	all	MG3S[80]
MR-MGM-BE4	SP	all	cc-pCVQZ (metal), aug-cc-pCVQZ (non-metal)
MR-MGN-BE17	SP	all	MG3S
SR-TM-BE15[d]	SP	3dSRBE4	def2-TZVP (metal), ma-TZVP (non-metal);
		SRMBE8	def2-TZVP;
		PdBE2	SDD-2fg (Pd), cc-pVTZ (non-metal);
		FeCl	aug-pwCVTZ (Fe), aug-pVTZ (Cl)
MR-TM-BE12[e]	SP	CuCl, NiCl, VO	aug-cc-pwCVTZ (metal), aug-cc-pVTZ (non-metal);
		3dMRBE6	def2-TZVP (metal), ma-TZVP (non-metal);
		MRBE3	def2-TZVP
MR-TMD-BE3	SP	V_2, Cr_2	def2-TZVP;
		Fe_2	def2-QZVP
HTBH38/18	SP	all	MG3S
NHTBH38/18	SP	all	MG3S
NCCE30/18	SP	all	MG3S
NGD21/18	SP	all	aug-cc-pVQZ
4pIsoE4	SP	all	cc-pVQZ
2pIsoE4	SP	all	cc-pVQZ
IsoL6/11	SP	all	MG3SXP[81]
πTC13	SP	all	MG3S
HC7/11	SP	all	6-311+G(2df,2p)
EA13/03	SP	all	MG3S
PA8	SP	all	MG3S
IP23	SP	Co, Cr, Cu, Mo, Pd, Rh, Ru, Sc, Zn	cc-pVTZ-DK;[82]
		FeC	SDD+2fg (Fe),[83] def2-QZVPP (C);[76]
		rest	MG3S
AE17	SP	H, He	cc-pV5Z;
		rest	cc-pwCV5Z
SMAE3/19	SP	all	MG3S
DC9/19	SP	all	MG3S
DGL6	Opt	all	6-311+G(2df,2p)[84]
DGH4	Opt	ZnS	B2 basis (Zn),[85] aug-cc-pVQZ (S);[86,87]
		HBr	aug-cc-pVQZ (H), jun-cc-pVQZ (Br);[88,79]
		NaBr	cc-pCVQZ (Na),[89] jun-cc-pVQZ (Br);
		Ag_2	jun-cc-pVTZ-PP (Ag)[90,79]
S6x6	SP	all	def2-QZVP
ABDE13	SP	all	ma-TZVP[91]

Database 2019 – excitation energies used for training			
3dEE8	SP	Ca^+	cc-pCVQZ;
		Fe_2	def2-QZVP;
		Fe, Mn^+, Ni^+, Sc, V, Zn	cc-pVQZ-DK
4dAEE5	SP	all	cc-pVTZ-DK
pAEE5	SP	Al, C^+, Si^+	cc-pVQZ-DK;
		F, Ar	d-aug-cc-pVQZ-DK[86]
EE23	SP	water	aug-cc-pVTZ;[87]
		B-TCNE	aug-cc-pVDZ;[87]
		DMABN, pNA	6-31+G**;[92]
		rest	jul-cc-pVTZ[87,79]
LRCTEE9	SP	all	jul-cc-pVTZ
Database 2019 – additional test data – ground-state properties			
Al2X6	SP	all	def2-QZVP
BHDIV10	SP	all	def2-QZVP
BHPERI26	SP	all	def2-QZVP
BHROT27	SP	all	def2-QZVP
DIPCS10	SP	all	def2-QZVP
HeavySB11	SP	all	def2-QZVP
PX13	SP	all	def2-QZVP
SIE4x4	SP	all	def2-QZVP
YBDE18	SP	all	def2-QZVP
S66x8	SP	all	def2-QZVP
MGBL193	Opt	all	aug-cc-pVTZ
TMBH22	SP	all	cc-pVQZ (B,C,H,O,N,Br), cc-pV(Q+d)Z (S,P,Cl), cc-pVQZ-PP (W,Mo,Re,Zr)
WCCR10	SP	all	def2-QZVPP
TSG48	Opt	all	MG3S
TMDBL10	Opt	all	def2-QZVP
DM79	Opt	all	def2-QZVP
PEC4	SP	all	aug-cc-pVQZ
ASNC2	SP	all	MG3S
NaCl	SP	all	aug-cc-pVQZ (Na), aug-cc-pV(Q+d)Z (Cl)
Database 2019 – additional test data – excitation energies			
EEA11	SP	Li, Be, Na, Mg, K	def2-QZVP;
		H, He, B, Ne, Al, Ar	aug-cc-pVQZ[86,87,*f*]
AEE15	SP	all	def2-TZVP
EEAroT5	SP	all	cc-pVDZ
EE69	SP	all	6-31(2+,2+)G(d,p)[93]
EER5	SP	all	6-31++G(d,p)
LRCTEE2	SP	$C_2H_4\cdots C_2F_4$	aug-cc-pVDZ;
		$F_2\cdots NH_3$	6-31+G**

[a] Opt indicates optimizations, and SP indicates single-point energy calculations.

[b] See the SI for complete lists of systems in each subdatabase.

[c] References for basis sets are specified at the first mention of each basis set.

[d] The subdatabases of the SR-TM-BE15 database are as follows. The 3dSRBE4 subdatabase contains $CrCl_2$, MnF_2, $FeCl_2$, and $CoCl_2$, the SRMBE8 subdatabase

contains Ag_2, AgH, $CrCH_3^+$, Cu_2, CuAg, $Cu(H_2O)^+$, VCO^+, and Zr_2, and the PdBE2 subdatabase contains $Pd(PH_3)_2$–C_6H_8 and $Pd(PH_3)_2$–$C_{10}H_{12}$-b.

[e] The subdatabases of the MR-TM-BE12 database are as follows. The 3dMRBE6 subdatabase contains TiCl, VF_5, CrCl, CrOF, $(FeBr_2)_2$, and $Co(CO)_4H$ and the MRBE3 subdatabase contains $NiCH_2^+$, $Fe(CO)_5$, and VS.

[f] The basis sets for atomic Rydberg states are the same as in Ref. 71; it is shown there that using double augmentation for Rydberg states would make the results worse.

4. Computational details

Software. All calculations presented in this work were performed using *Gaussian 09*,[94] *Gaussian 16*,[95] or Minnesota–Gaussian Functional Module[96] (*MN-GFM6.10*), which is a locally modified version of *Gaussian 09*.

Grids. The UltraFine grid, which is a pruned (99, 590) grid with 99 radial shells and 590 angular points per shell, was used for most of the calculations. For two cases, namely M11 and MN12-SX calculations on SH_3^+ in the MGBL193 database, a finer grid (–96032) was used.

Stability. The stability of the wave function was checked for all the databases in the training set of Database 2019 (both during and after optimization) except for EE23 and LRCTEE9 and for the ground-state databases of the additional test data of Database 2019, and if the wave function was found to be unstable, it was further optimized until it converged to a minimum-energy stationary point.

Geometries. Calculations on all the databases were single-point calculations except for the geometry databases and the dipole moment database – those were consistently optimized with each functional. The geometries used for the single-point calculations may be found in the references given in Tables 2 and 3.

Zero-point energy. For ground-state properties, all the energies calculated in this work are Born–Oppenheimer energies (total electronic energy including nuclear repulsion at a fixed geometry) and do not include zero-point vibrational energy (ZPVE). Hence, for reference data that are obtained from experiments, zero-point vibrational energy and thermal contributions due to vibrational and rotational energies were removed, if present. Among excited-state properties databases, only the AEE15 database includes ZPVE. For this database, the ZPVE values for the ground-state and excited-state structures were obtained using B3LYP in Ref. 72, and these values are used in this work for all density functionals.

Spin-orbit coupling. For databases in the training set of Database 2019 with experimental reference values, we compare calculated values to experimental values by adding spin-orbit coupling (SOC) to the calculated values. For the additional test data of Database 2019 and when the reference values were from high-level theoretical calculations without SOC, we omitted SOC in the density functional calculations. The databases for which SOC was added to at least one species (in a reaction database this can be reactant(s) and/or the product(s)) are SR-MGM-BE8, SR-MGN-BE107, SR-TM-BE15, MR-MGM-BE4, MR-MGN-BE17, MR-TM-BE12, MR-TMD-BE3, IP23, EA13/03, 3dAEE8, 4dAEE5, pEE5, DC9/19, DGL6, and SMAE3/19. See page S-11 of the Supporting Information of Ref. 18 for further discussion of spin-orbit energies and see Table S19 of that Supporting Information for SOC values of the species involved in these databases.

AE17. The AE17 database is a special case and is an exception to our usual procedure. Whereas the reference data in all other databases are best estimates of electronic energies, including relativistic effects (which are always present in experimental data), the reference values in the AE17 database are best estimates of absolute nonrelativistic atomic energies. They were obtained[41] by removing relativistic effects from experimental ionization potentials. Thus, our comparisons to this data are entirely nonrelativistic – no spin-orbit energy and no scalar relativistic effects.

Scalar relativistic effects. Most of the calculations tested in this work are nonrelativistic calculations. When scalar relativistic effects are included, it is done either by using relativistic effective core potentials for heavy elements or by using all-election calculations with the second-order Douglas–Kroll–Hess (DKH) method.[97] When the DKH Hamiltonian is used, one must use basis sets specially developed for this purpose; such basis sets have a suffix "–DK" in Table 4. The databases for which relativistic effects were taken into consideration for one or more species in the database by using the DKH Hamiltonian and DK basis sets are: IP23, 3dAEE8, 4dAEE5, and pEE5. The databases (and species or atoms) for which relativistic effects were taken into consideration for one or more species in the database by using relativistic effective core potentials are SR-TM-BE15 (Pd), IP23 (Fe), DGH4 (Zn, Ag), TMBH22 (W, Mo, Re, Zr), WCCR10 (Ru, Pd, Ag, Pt, Au), TMDBL10 (Pd, Ag, Pt, Au), and DM79 (Rb, Sr, Y, Zr, I, La, Hf, Tl, Pb).

Excited states. There are three types of excited-state energy calculations in this work. The first type is ΔSCF, in which method the excitation energy is the difference in the energies of ground-state and excited-state SCF calculations, where both states are converged to a stable solution; this method is limited to cases where the ground and excited states have different symmetries. The

excitation energies for the 3dEE8, 4dAEE5, and pAEE5 databases are calculated using the ΔSCF method, which involves performing two SCF calculations (one for the ground state and another one for the excited state) and taking the energy difference of the ground state and the excited state to be the excitation energy. In the second type, we do linear-response time-dependent DFT (LR-TDDFT) calculations, wherein vertical excitation energy for the desired state is obtained. Note that stability check was not performed with LR-TDDFT calculations. All the excitation energies for the EE23 and LRCTEE9 databases in the training set and the EEA11, EEAroT5, EE69, EER2, and LRCTEE2 databases in the additional test data of Database 2019 were treated using LR-TDDFT. The third type of calculation yields adiabatic excitation energies. The adiabatic excitation energies of AEE15 for the desired state were obtained by adding three quantities: (a) the energy difference between excited-state and ground-state structures (with structures obtained by B3LYP in Ref. 72), (b) the energy difference between the ZPVE values of the excited-state and ground-state structures, and (c) LR-TDDFT vertical excitation energy on the excited-state structure.

Solvent effect. Almost all of the reference data is gas-phase data. There is one exception. For one of the complexes of EEAroT5, anthracene-TCNE, the experimental value is in solution phase, and we estimated the solution-phase result by subtracting 0.32 eV[53] from our calculated values.

Counterpoise correction. No counterpoise corrections were used in any of the calculations of this paper.

5. Exchange–correlation functionals tested for comparison

Because revM11 is a range-separated hybrid functional, in this work, we compare the performance of revM11 to ten previously published range-separated hybrid functionals. These include

- screened-exchange functionals (HSE06,[98,99] N12-SX,[100] and MN12-SX[100]) for which the percentage X of HF exchange decreases monotonically from a finite value at short interelectronic separations to zero at long interelectronic separations,
- middle-range functional (HISS[101,102]) for which X increases from zero to a finite value at medium interelectronic separations and then decreases to zero at long interelectronic separations, and
- long-range corrected functionals (M11, LC-ωPBE,[103] ωB97,[104] ωB97X,[104] and ωB97X-D[105]) for which X increases monotonically from zero or a finite value at short interelectronic separations to 100% at long interelectronic separations.

- the CAM-B3LYP[106] functional, for which *X* increases monotonically with increase in interelectronic separation, but not all the way up to 100% at long interelectronic separations.

Besides range-separated hybrid functionals, we also compare the performance of revM11 to popular local functionals (PBE,[107] BLYP,[108,109] TPSS,[110] and M06-L[41]) and popular global hybrid functionals (B3LYP,[111] PBE0,[112] M06,[13] and M06-2X[13]). Additionally, four recently developed functionals, two of which are local (MN15-L and revM06-L) and two of which are global hybrids (MN15 and revM06), are also tested. All the functionals tested in this work are listed in Table 5 along with their type and percentage of HF exchange.

Note that all functionals in the present tests have local correlation. The hybrid functionals have nonlocal exchange, and the non-hybrid functionals are completely local. (Note that some researchers use the word "semilocal" where we and many other chemists use "local".)

Table 5. Exchange–correlation functionals tested in this work.

Type[a]	Functional	*X* [ω][b]	Reference(s)	Year
GGA	BLYP	0	108,109	1988
	PBE	0	107	1996
meta-GGA	TPSS	0	110	2002
	M06-L	0	41	2006
	revM06-L	0	17	2017
meta-NGA	MN15-L	0	15	2016
global hybrid GGA	B3LYP	20	111	1993
	PBE0	25	112	1996
global hybrid meta-GGA	M06	27	13	2008
	M06-2X	54	13	2008
	revM06	40.41	18	2018
global hybrid meta-NGA	MN15	44	16	2016
RS hybrid[c]	CAM-B3LYP	19–65	106	2004
	HSE06	25–0	98,99	2006
	LC-ωPBE	0–100 [0.4]	103	2006
	HISS	0–60–0	101,102	2007
	ωB97	0–100 [0.4]	104	2008
	ωB97X	15.7706–100 [0.3]	104	2008
	ωB97X-D	22.2036–100 [0.2]	105	2008
	M11	42.8–100 [0.25]	8	2011
	N12-SX	25–0	100	2012
	MN12-SX	25–0	100	2012
	revM11	22.5–100 [0.40]	this work	2018

[a]GGA = generalized-gradient approximation; meta-GGA = GGA plus local kinetic energy density; meta-NGA = nonseparable gradient approximation plus local kinetic energy density; hybrid-GGA = GGA plus some percentage of nonlocal HF exchange; hybrid-meta-GGA = GGA plus local kinetic energy density and some percentage of nonlocal HF exchange; hybrid-meta-NGA = NGA with local kinetic energy density and some percentage of nonlocal HF exchange; RS = range-separated
[b]X is the percentage of Hartree–Fock exchange. A single value indicates a local functional if $X = 0$ or a global hybrid if $X \neq 0$; a range with two values indicates X at short and long interelectronic separations (in that order); and a range with three values indicates X at short, medium, and long interelectronic separations. For long-range-corrected functionals, we also list the range parameter ω, which has units of a_0^{-1}, where 1 a_0 = 1 bohr = 0.529177 Å.

6. The revM11 functional

The revM11 functional is obtained by reoptimizing the M11 functional[8] with the following differences: (i) we optimized the nonlinear range parameters mainly by using the excited-state databases of the training set of Database 2019; (ii) we optimized the linear parameters mainly by using the ground-state databases of the training set of Database 2019, which is larger and more diverse than the database used for M11, (iii) we added smoothness restraints, and (iv) we deleted some higher-order terms that did not contribute significantly to the accuracy.

The equations that describe the revM11 functional are the same as the equations of M11 with the exception already mentioned that some terms are dropped. Since the original M11 functional form is fully described in a previous paper,[8] here we simply review the key elements. The functional form of the revM11 exchange-correlation functional may be separated into three terms:

$$E_{xc}^{\mathrm{revM11}} = \left(\frac{X_0}{100}\right) E_x^{\mathrm{HF}} + \left(1 - \frac{X_0}{100}\right)(E_x^{\mathrm{LR-HF}} + E_x^{\mathrm{SR-revM11}}) + E_c^{\mathrm{revM11}} \quad (1)$$

where E_x^{HF} is the full-range nonlocal Hartree-Fock exchange, and both the local exchange $E_x^{\mathrm{SR-revM11}}$ and the local correlation E_c^{revM11} depend on the spin-specific densities (i.e., the up-spin density ρ_α and the down-spin density ρ_β), their gradients, and the spin-specific kinetic energy densities (τ_σ), with $\sigma = \alpha$ or β.

The local exchange term consists of the short-range revM11 exchange functional ($\left(1 - \frac{X_0}{100}\right) E_x^{\mathrm{SR-revM11}}$). The $E_x^{\mathrm{SR-revM11}}$ term involves two polynomials with coefficients a_i^x, and b_i^x. The nonlocal exchange term consists of short-range HF exchange ($\frac{X_0}{100} E_x^{\mathrm{SR-HF}}$) and long-range HF exchange ($E_x^{\mathrm{LR-HF}}$), where the former equals to $\frac{X_0}{100}(E_x^{\mathrm{HF}} - E_x^{\mathrm{LR-HF}})$. The correlation term involves two polynomials with coefficients a_i^c, and b_i^c.

The long-range HF exchange term ($E_x^{\mathrm{LR-HF}}$) is calculated by the Hartree-Fock expression for the exchange energy of the Kohn-Sham determinant but with the replacement

$$\left.\frac{1}{r_{12}}\right|_{\text{in long-range term}} \rightarrow \frac{\mathrm{erf}(\omega r_{12})}{r_{12}} \tag{2}$$

where r_{12} is the interelectronic separation, ω is the range-separation parameter, and erf is the error function, which increases zero to one as r_{12} increases from 0 to ∞. This operator is nonsingular but long-ranged, and it increases more rapidly when ω is larger.

7. Optimization scheme

The parameters X_0 and ω were determined based on a preliminary analysis of the performance achievable for the EE23, LRCTEE9, and ground-state databases. Given trial values of X_0 and ω, we optimized the linear parameters with the training set of Database 2019 by using a preliminary set of inverse weights on the subdatabases. Using those linear parameters with the given X_0 and ω, we then tested excited states. We then varied X_0 and ω and repeated this procedure until we got good results for all kinds of excited states. Then, having selected X_0 and ω, we varied the weights on the databases in the training set until we got the best possible across-the-board behavior. We then tested the final functional on both the training data and the additional test data. Once X_0 and ω were final, the optimization of linear polynomial coefficients a_i^x, b_i^x, a_i^c, and b_i^c (all defined precisely in the original M11 article[8]) was performed using the training set of Database 2019 that do not involve TDDFT calculations. There are 29 such databases (see Table 2). Each optimization round involved a new set of SCF calculations to update the Kohn–Sham Slater determinant representing the density. After a few trials, the numbers of terms in each of the four polynomials (with coefficients a_i^x, b_i^x, a_i^c, and b_i^c) was set to seven. This may be compared to eleven terms in each polynomial in M11. Therefore, the number of linear parameters in revM11 is 4×7 = 28, but there are six physical constraints (discussed next), which reduces the number of free linear parameters to 22.

During the optimization process, six constraints are maintained – two of them are on exchange, two of them are on correlation, and two of them are on kinetic energy density exchange enhancement factors. The constraints are the same as in the M11 functional and are explained in the M11 paper.[8] The two constraints on kinetic energy density exchange enhancement factors given by

eqs. 21 and 22 in the M11 paper[8] have typos and the correct equations should have the factor (1 – *Y*) deleted.

The optimization of the 28 linear parameters in revM11 was done by minimizing a training function, *F*, which is given by

$$F = \sum_{n=1}^{29} \frac{R_n}{I_n} + \lambda(a + b + c + d) \quad (3)$$

where

R_n = root mean squared error of database n in the training set of Database 2019,

I_n = inverse weight of database n,

$a = \sum_{i=0}^{6}(a_i^x - a_{i+1}^x)^2$,

$b = \sum_{i=0}^{6}(b_i^x - b_{i+1}^x)^2$,

$c = \sum_{i=0}^{6}(a_i^c - a_{i+1}^c)^2$,

$d = \sum_{i=0}^{6}(b_i^c - b_{i+1}^c)^2$, and

λ is a parameter.

The terms multiplied by λ in eq (3) constitute a smoothness restraint, and a higher value of λ increases the smoothness of the functional, albeit at the cost of deteriorating the performance of the functional for minimizing R_n. The value of λ used here is 0.02, which is higher than that used in our recent functionals,[15,16,17,18] and for this reason, as well as because we decreased the order of the polynomials, we expect the revM11 functional to be smoother than our other recent functionals.

8. Parameters of revM11

The 28 parameters in the last 14 rows of Table 6 were optimized on the same training set that was used in our recent work on the revM06[18] functional plus the S6x6 and ABDE13 databases. This training set has only atomic and molecular properties databases with energies and geometries of various systems. The values of X_0 and ω were tuned mainly for excitation energies, the parameter λ was chosen to promote smoothness of the functional, and the linear parameters were chosen to minimize the functional in eq 3.

In going from M11 to revM11, the percentage of HF exchange at short interelectronic separations, X_0, is changed from 42.8% to 22.5% and the range-separation parameter, ω, is changed from 0.25 a_0^{-1} to 0.40 a_0^{-1}. The percentage of HF exchange in the limit of large interelectronic separations was not changed, and it remains at 100%.

Efforts were made to make the revM11 functional smoother than our recent functionals by increasing the smoothness restraint, λ from 0.01 to 0.02. Other higher values of λ such as 0.05 were also tested but this led to significant worsening of a number of ground-state properties. Hence, to get a balance between having a smooth functional obtaining good performance on various properties, we use $\lambda = 0.02$.

All the optimized parameters are given in Table 6. A Fortran version of revM11 is in the *MFM* program, version 4.0, available for free download at https://comp.chem.umn.edu/mfm.[113]

Table 6. The optimized exchange and correlation parameters of the revM11 functional.

parameter	exchange[a]	correlation
ω	0.40	
X_0	22.5	
a_0	–0.3288860885	1.0000000000
a_1	–8.3888150476	0.0000000000
a_2	0.7123891057	–0.7860212983
a_3	3.6196212952	–5.1132585425
a_4	4.3941708207	–4.0716488878
a_5	5.0453345584	1.5806421214
a_6	7.8667061191	8.4135687567
b_0	1.1038860885	0.9732839024
b_1	8.0476369587	–2.1674450396
b_2	–0.7353624773	–9.3318324572
b_3	–2.4735275550	–12.9399606617
b_4	–4.7319060355	–2.2129320660
b_5	–5.8502502096	–2.9508549100
b_6	–7.5059975327	–1.5066319360

[a]Note that, for the exchange part, the parameters a_0 to b_6 were optimized such that they need to be multiplied by factor $(1 - X_0/100)$, where $X_0 = 22.5$. Therefore, in the table above and in our code,[96] the factor $(1 - X_0/100)$ is included with the parameters. However, in Table 1 of the M11 paper[8] the parameters were presented without the factor $(1 - X/100)$, in the notation of that paper, multiplied into them.

9. Results and discussion

In the subsections that follow, we show the performance of the revM11 functional, and we compare the results to those for 22 other density functionals on 56 databases of which 31 databases are in the training set of Database 2019 (see Table 2) and 25 databases are in the additional test data of Database 2019 (see Table 3). These two subsets of Database 2019 are further subdivided into ground-state and excited-state databases. The results of some of the comparison functionals on

some of these databases were presented in our very recent work on density functional optimization,[15,16,17,18] but we present them here again for easy comparison of functionals for a given database. If some results for some databases were already presented in references other than Refs.15, 16, 17, and 18, those references are specifically mentioned in the associated subsection.

The mean unsigned errors (MUEs) on the 31 databases in the training set of Database 2019 are reported in Tables 7 and 8, where Table 7 gives results for range-separated hybrid functionals and Table 8 gives results for local and global hybrid functionals. Tables 7 and 8 also have a mean unsigned error over 467 atomic and molecular energies (AME467), as explained in footnotes to these tables. Notice that density functionals in the remaining tables are always listed in the same order as in Table 5.

Table 7. Mean unsigned errors on the training set of Database 2019 with 11 range-separated hybrid functionals.

Databases[a]	CAM-B3LYP	HSE06	LC-ωPBE	HISS	ωB97	ωB97X	ωB97X-D	M11	N12-SX	MN12-SX	revM11
Ground-state energetics											
SR-MGM-BE8	3.4	3.7	3.2	3.5	3.4	3.1	2.5	5.9	1.9	4.5	2.6
SR-MGN-BE107	1.8	1.9	2.1	2.4	1.2	1.2	1.1	0.9	1.5	1.0	1.5
SR-TM-BE15	4.9	3.3	7.4	5.3	5.6	4.3	2.5	7.3	4.4	10.0	5.4
MR-MGM-BE4	10.5	8.5	14.0	5.3	8.3	11.9	9.5	11.2	8.3	9.2	6.7
MR-MGN-BE17	6.8	5.3	8.2	9.0	7.7	7.1	6.3	7.0	6.1	4.4	5.6
MR-TM-BE12	5.0	5.0	4.5	8.7	5.0	4.8	4.0	6.9	3.3	8.6	4.7
MR-TMD-BE3	65.5	65.0	75.8	50.4	53.8	62.0	60.9	83.2	20.4	23.0	48.7
HTBH38/18	3.4	4.6	1.1	1.4	1.9	2.1	2.6	1.4	4.1	0.9	1.8
NHTBH38/18	2.6	3.6	2.3	1.6	2.3	2.9	3.7	1.3	2.7	1.3	2.0
NCCE30/18	0.79	0.88	1.02	0.59	0.47	0.45	0.36	0.28	0.85	0.44	0.38
NGD21/18	0.15	0.10	0.23	0.10	0.10	0.03	0.16	0.14	0.26	0.27	0.04
S6x6	2.52	2.36	2.83	2.16	0.82	1.07	0.31	0.63	2.52	1.29	0.52
IP23	4.7	3.9	6.6	4.1	4.6	3.9	2.9	7.9	4.3	6.9	4.0
EA13/03	2.1	2.7	2.1	3.1	2.5	2.0	1.8	1.0	2.9	2.1	1.9
PA8	1.4	1.1	1.8	2.1	1.8	1.5	2.4	1.0	2.0	1.2	1.4
2pIsoE4	3.2	2.4	1.1	2.2	0.9	1.5	1.9	1.9	2.6	2.0	0.9
4pIsoE4	3.9	2.6	1.4	2.6	1.9	2.4	2.5	2.5	2.0	2.7	1.7
IsoL6/11	2.1	1.2	1.9	1.5	1.5	1.6	1.1	1.1	1.8	1.2	2.3
πTC13	3.7	6.2	4.3	7.1	3.9	4.4	6.2	2.2	7.9	3.2	1.6
AE17	11.0	32.8	25.1	23.6	6.3	5.7	5.7	9.1	10.5	4.1	5.0
HC7/11	6.2	7.3	17.7	15.2	11.5	6.8	4.6	3.7	11.0	2.2	10.9
SMAE3/19	2.6	2.5	2.3	4.5	2.1	1.7	1.5	2.0	0.8	0.9	1.1
DC9/19	3.1	3.6	2.3	1.6	3.1	1.7	3.0	1.9	2.4	1.6	2.7
ABDE13	4.9	4.9	3.7	4.1	0.8	1.1	1.5	2.3	1.9	1.6	2.1
Ground-state bond distances											
DGL6	0.008	0.003	0.013	0.010	0.011	0.008	0.005	0.007	0.005	0.003	0.009
DGH4	0.010	0.016	0.012	0.014	0.019	0.017	0.023	0.018	0.011	0.017	0.010
Excitation energies											
3dEE8	8.3	12.9	12.0	10.2	13.8	10.0	8.3	14.5	17.7	23.4	9.3
4dAEE5	6.2	5.7	5.7	6.2	5.7	8.8	7.0	5.8	6.2	16.2	4.8
pAEE5	2.6	5.5	8.0	7.4	9.9	5.9	8.1	5.3	10.8	7.9	1.8
EE23	0.37	0.41	0.33	0.47	0.34	0.25	0.30	0.35	0.46	0.68	0.33
LRCTEE9	2.84	5.47	0.56	4.57	0.49	1.07	2.13	1.08	5.61	5.13	0.39
467 atomic and molecular energies (AME467)											
AME467[b]	3.7	4.7	4.6	4.3	3.2	3.0	2.9	3.3	3.6	3.0	2.7

[a]The unit for all the databases is kcal/mol except for DGL6 and DGH4, which are in Å and for EE23 and LRCTEE9, which are in eV.

[b]AME467 is a subdatabase of 467 atomic and molecule energies. It includes all the data in the subdatabases of Table 2 except for DGL6, DGH4, EE23, and LRCTEE9. This row of the table contains the MUE of AME467. It can be computed as the unweighted MUE over its 467 data or as the weighted average of its 27 subdatabase MUEs, with each MUE weighted by the number of data in the subdatabase.

Table 8. Mean unsigned errors on the training set of Database 2019 with 12 local and global hybrid functionals.

Databases[a]	BLYP	PBE	TPSS	M06-L	revM06-L	MN15-L	B3LYP	PBE0	M06	M06-2X	revM06	MN15
Ground-state energetics												
SR-MGM-BE8	4.9	2.5	3.0	3.8	2.5	2.6	4.4	3.7	4.1	1.6	1.8	1.6
SR-MGN-BE107	2.6	3.4	2.3	2.0	1.8	1.5	2.2	1.9	1.2	0.7	1.0	0.9
SR-TM-BE15	4.8	5.4	4.0	4.4	5.4	3.0	4.4	3.1	2.8	6.6	2.8	2.9
MR-MGM-BE4	8.7	9.3	6.7	11.9	6.4	1.9	7.8	8.9	5.0	10.4	6.4	3.9
MR-MGN-BE17	6.7	14.8	4.2	3.0	2.3	2.1	5.1	5.2	4.1	5.7	4.2	2.8
MR-TM-BE12	10.3	10.2	6.5	3.5	3.8	3.1	4.8	4.9	3.6	12.4	5.7	4.1
MR-TMD-BE3	31.4	18.7	12.3	6.5	20.8	20.9	27.8	68.6	36.7	120.0	43.5	22.8
HTBH38/18	7.9	9.7	8.1	4.6	2.0	1.3	4.5	4.6	2.4	1.3	1.5	1.1
NHTBH38/18	8.5	8.4	8.9	3.7	2.2	2.0	4.5	3.3	2.3	1.2	1.1	1.7
NCCE30/18	1.88	1.43	1.42	0.65	0.61	0.81	1.25	0.84	0.49	0.34	0.38	0.39
NGD21/18	0.38	0.10	0.17	0.13	0.07	0.02	0.28	0.11	0.19	0.11	0.04	0.02
S6x6	4.96	2.61	3.52	0.80	0.79	1.72	3.78	2.44	1.12	0.54	0.55	0.34
IP23	6.4	6.0	4.1	3.9	4.5	2.5	5.3	3.3	5.0	3.4	3.1	2.5
EA13/03	2.7	2.2	2.3	3.8	5.4	2.1	2.3	2.7	1.8	2.1	1.6	0.9
PA8	1.6	1.3	2.7	1.9	2.6	2.2	1.0	1.2	1.8	1.6	1.6	1.1
2pIsoE4	5.5	2.7	3.5	3.2	4.4	2.0	4.7	2.2	1.6	1.8	1.9	0.3
4pIsoE4	4.0	2.4	2.6	2.9	5.9	3.8	4.2	2.3	2.3	2.7	2.4	2.0
IsoL6/11	3.7	2.0	3.7	2.8	1.3	1.3	2.6	1.4	1.3	1.5	1.0	1.8
πTC13	6.1	5.6	8.1	6.7	7.0	4.8	6.0	6.1	4.4	1.5	2.8	3.5
AE17	8.4	47.3	18.1	7.0	4.5	7.5	18.3	38.6	4.5	2.2	3.9	6.8
HC7/11	27.4	4.0	10.5	3.4	3.5	4.0	16.8	9.4	2.8	2.1	2.4	3.7
SMAE3/19	1.4	4.4	2.0	1.1	1.2	1.1	3.5	2.0	0.4	2.0	0.8	0.1
DC9/19	8.2	6.5	6.2	3.7	2.7	2.8	6.2	3.5	2.0	2.3	1.8	2.3
ABDE13	12.0	5.1	10.7	5.4	2.4	4.6	8.6	4.3	2.3	1.4	1.3	1.8
Ground-state bond distances												
DGL6	0.019	0.013	0.010	0.006	0.009	0.004	0.009	0.003	0.006	0.004	0.008	0.005
DGH4	0.040	0.021	0.014	0.009	0.009	0.024	0.028	0.014	0.022	0.048	0.018	0.011

Excitation energies												
3dEE8	12.8	9.0	9.8	7.2	8.3	3.9	9.4	10.3	9.9	7.6	7.7	9.2
4dAEE5	6.3	5.3	5.8	7.2	5.0	1.1	6.3	5.3	7.3	9.3	3.9	5.9
pAEE5	4.9	3.7	2.0	7.7	7.3	5.0	2.6	5.5	5.5	4.8	4.5	4.5
EE23	0.86	0.81	0.69	0.55	0.56	0.34	0.50	0.40	0.66	0.23	0.35	0.34
LRCTEE9	7.25	7.23	7.03	6.73	6.38	6.17	5.47	4.98	4.88	2.70	3.73	3.58
467 atomic and molecular energies (AME467)												
AME467[b]	5.7	6.7	5.1	3.2	2.8	2.3	4.6	4.8	2.6	2.9	2.1	2.0

[a] The unit for all the databases is kcal/mol except for DGL6 and DGH4, which are in Å and for EE23 and LRCTEE9, which are in eV.

[b] AME467 is a subdatabase of 467 atomic and molecule energies. It includes all the data in the subdatabases of Table 2 except for DGL6, DGH4, EE23, and LRCTEE9. This row of the table contains the MUE of AME467. It can be computed as the unweighted MUE over its 467 data or as the weighted average of its 27 subdatabase MUEs, with each MUE weighted by the number of data in the subdatabase.

9.1 Performance for excited-state properties

9.1.1 Performance on excitation energies of subdatabases in Table 2

The excited-state databases used in training the revM11 functional are 3dEE8, 4dAEE5, pAEE5, EE23, and LRCTEE9. The 3dEE8, 4dAEE5, and pAEE5 databases are treated by the ΔSCF method and were the only excited state databases used in the optimization of our functionals in recent work[15,16,17,18] Here, for training the new functional, we include two more databases (EE23 and LRCTEE9) that were not part of our past work. The excitation energies for these two databases are obtained from linear response time-dependent density functional theory calculations. Each of the five databases is discussed in detail below.

Excitation energies calculated using TDDFT calculations. The values of X_0 and ω give the amount of HF exchange in the revM11 functional at various interelectronic distances, and they were determined mainly based on the performance of revM11 on EE23 and LRCTEE9 databases; although in finalizing these two parameters the performance of revM11 on training sets involving ground-state properties was also taken into account.

The EE23 database represents a diverse set of vertical electronic excitations of 19 molecules: 18 valence excitation energies (VEE18), two Rydberg excitation energies (REE2), and three intramolecular and intermolecular charge transfer excitations (CTEE3), and therefore, it is a good database for testing the performance of quantum mechanical methods on various types of excitations. Because CTEE3 contains only short-to-medium range CT excitations, we also include the LRCTEE9 database, which has nine long-range charge transfer excitations, in particular, the $\pi \rightarrow \pi^*$ $^1A_1$ excitations of the $NH_3\cdots HNO_2$ complex at nine intermonomer distances (3.6772, 6.1133, 8.5632, 11.0156, 13.4708, 15.9272, 18.3868, 23.3034, and 25.7630 Å), where none of the distances are equilibrium distances.

In Tables 7 and 8, the MUE reported for EE23 database is the average MUE over MUE (VEE18), MUE (REE2), and MUE (CTEE3) with the three subdatabases of EE23 weighted equally. We find that the best performance is by M06-2X with an MUE of 0.23 eV and the second best is by ωB97X with an MUE of 0.25 eV; revM11 improves negligibly over M11 and is the third best functional amongst 11 range-separated hybrid functionals of Table 7. All local density functionals give large errors, and Rydberg and/or CT excitations dominate the error in every case.

The LRCTEE9 database is very interesting as it allows us to see long-range charge transfer excitations up to intermonomer distances as long as ~26 Å, and previous work[75,114] has shown that

the type of functionals that do well for short-to-medium range CT excitations may or may not work well for this kind of excitation. Tables 7 and 8 show that the M06-2X, ωB97X, and ωB97X-D functionals, which are the best, second best, and the third best for EE23, give MUEs of 2.70, 1.07, and 2.13 eV, respectively, for LRCTEE9, all of which are above 1 eV and can therefore be deemed unsuitable for long-range charge transfer excitations. Therefore, it was a major objective of the present reparametrization to do well for this database. Of the 23 functionals tested in Tables 7 and 8, only three functionals give an MUE less than 1 eV for LRCTEE9 – these are revM11, LC-ωPBE, and ωB97, all of which are long-range corrected hybrid functionals that have $\omega = 0.4\ a_0^{-1}$. Table 7 shows though that simply having 100% HF exchange at long range is insufficient to ensure good predictions for LRCTEE9; rather the HF exchange must increase rapidly to its asymptotic value. Thus Table 7 shows that the long-range corrected functionals M11, ωB97X, and ωB97X-D, each of which has $\omega \leq 0.3\ a_0^{-1}$, all yield an MUE greater than 1 eV. The revM11 functional not only improves significantly over M11 but also has the smallest MUE (= 0.39 eV) among the 23 tested density functionals; the second and third best functionals being ωB97 and LC-ωPBE, respectively. The good performance of revM11 for LRCTEE9 is particularly noteworthy because obtaining good performance for this database required a Hartree-Fock exchange profile that increases rapidly with interelectronic separation, and this then presents a challenge in obtaining good performance for both excited-state and ground-state systems with high static correlation; this is a good example of how obtaining good performance in one kind of test makes it harder to obtain good performance in some other tests.

3d excitation energies. The 3d excitation energies database, 3dEE8, has seven atomic excitation energies and one molecular excitation energy. The subset of seven atomic excitation energies is referred to as 3dAEE7 and the one molecular case is the first excitation energy of Fe_2 dimer. One of the seven atomic excitation energies, namely Ca^+, is not 3d transition metal; but Ca^+ is interesting because its first excitation energy is a doublet-to-doublet transition from a 4s to a 3d orbital. (Note that the second excitation energy of Ca^+ is a $4s \rightarrow 4p$ transition). Except for Ca^+, all the excitations involve change in spin multiplicity from the ground spin state to the excited spin state. The 3dEE8 database has more challenging systems than the 4dAEE5 and pAEE5 databases, and Table 7 shows that for this database revM11 has MUE = 9.3 kcal/mol, which is a significant improvement over M11 with MUE = 14.5 kcal/mol.

4d atomic excitation energies. The 4d atomic excitation energies database, 4dAEE5, comprises atomic excitation energies of five 4d atoms/ions, Mo^+, Pd, Rh^+, Ru^+, and Y^+. All five excitations involve a change in spin multiplicity from the ground spin state to the excited spin state. From Tables 7 and 8, we see that the revM11 functional is the third best functional for 4dAEE5, trailing only the MN15-L and revM06 functionals, and it improves over M11 by 1.0 kcal/mol.

p-block atomic excitation energies. The p-block atomic excitation energies database, pAEE5, comprises atomic excitations of five p-block atoms and ions: Al, Ar, C^+, F, and Si^+. All five excitations involve a change in spin multiplicity from the ground spin state to the excited spin state. The revM11 functional has the smallest MUE, 1.8 kcal/mol, for pAEE5 (see Tables 7 and 8) and it also improves significantly over M11, which has an MUE of 5.3 kcal/mol.

9.1.2 Performance on excitation energies of subdatabases in Table 3

The excitation energy databases of the additional test data of Database 2019 are EEA11, AEE15, EEAroT5, EE69, EER5, and LRCTEE2. The results obtained with 16 density functionals for these databases are summarized in Table 9.

Table 9. Mean unsigned errors (in eV) for excitation energies on the additional test data of Database 2019 using 16 density functionals.

Functional	EEA11			AEE15	EEAroT5	EE69			EER5	LRCTEE2
	val[a]	Ryd[b]	val + Ryd[c]	val[a]	CT[d]	val[a]	Ryd[b]	val + Ryd[c]	CT[d]	CT[d]
PBE	0.12	1.32	0.77	0.38	1.79	0.43	1.38	0.97	0.95	6.65
B3LYP	0.15	0.82	0.52	0.21	1.38	0.23	0.85	0.58	0.55	4.77
M06-2X	0.30	0.85	0.60	0.34	0.53	0.36	0.26	0.30	0.15	2.10
revM06	0.17	0.75	0.49	0.30	0.89	0.33	0.25	0.29	0.28	3.03
MN15	0.24	0.81	0.55	0.35	0.79	0.28	0.24	0.26	0.22	2.98
CAM-B3LYP	0.14	0.71	0.45	0.24	0.55	0.34	0.31	0.32	0.27	2.44
HSE06	0.11	0.68	0.42	0.24	1.33	0.25	0.57	0.43	0.56	4.59
LC-ωPBE	0.16	0.71	0.46	0.33	0.34	0.44	0.35	0.39	0.78	0.59
HISS	0.13	0.53	0.35	0.27	1.05	0.43	0.23	0.31	0.41	3.57
ωB97	0.19	0.66	0.45	0.35	0.37	0.45	0.39	0.41	0.82	0.53
ωB97X	0.17	0.68	0.45	0.31	0.08	0.40	0.28	0.33	0.65	0.98
ωB97X-D	0.18	0.85	0.54	0.28	0.49	0.32	0.28	0.30	0.45	1.96
M11	0.21	0.92	0.60	0.35	0.07	0.37	0.59	0.49	0.60	0.88
N12-SX	0.33	0.91	0.65	0.24	1.37	0.25	0.85	0.59	0.56	4.60
MN12-SX	0.53	1.47	1.04	0.29	1.28	0.39	1.90	1.24	0.54	4.47
revM11	0.12	0.82	0.50	0.30	0.38	0.38	0.24	0.30	0.71	0.40

[a]MUE over valence excitations.

[b]MUE over Rydberg excitations.

[c]MUE over all the excitations (valence + Rydberg) of EEA11 or EE69 database.
[d]MUE over charge-transfer (CT) excitations.

The EEA11 database has valence excitations of five atoms (Li, Be, Na, Mg, and K) and Rydberg excitations six of atoms (H, He, B, Ne, Al, and Ar). The valence excitations of atoms are excitations in which the principal quantum number does not increase, and the Rydberg excitations considered here are excitations in which the principal quantum number increases by 1. The MUEs in Table 9 show that a middle-range hybrid functional, HISS, has the smallest MUE over the 11 excitations, and its good performance is due to Rydberg excitations because many functionals in Table 9 do well for valence excitations. We see that revM11 shows improvement over M11, and its performance is similar to the LC-ωPBE and ωB97X-D range-separated hybrid functionals.

The AEE15 database is a representative database of a set of 109 adiabatic excitation energies which were presented in Ref. 72. It consists of 15 adiabatic valence excitation energies of 15 systems that represent a variety of kinds of systems – organic and inorganic molecules and radicals. Unlike other TDDFT based excitation energies databases in this work, which involve vertical excitations, this one involves adiabatic excitations. Almost every functional in Table 9 gives an MUE in the range 0.25—0.35 eV and revM11 lies in the middle of this range with an MUE of 0.30 eV. Additionally, revM11 improves over M11 by 0.05 eV.

The EEAroT5 database consists of excitation energies of five charge-transfer molecular complexes taken from Ref. 53. These complexes involve an aromatic donor (Ar = benzene, toluene, o-xylene, naphthalene, and anthracene) and an organic acceptor, tetracyanoethylene (TCNE). The geometries of all the five complexes are the same as those provided in Ref. 53 and these equilibrium geometries, which were obtained with B3LYP/cc-pVDZ, are used to do single-point LR-TDDFT calculations with all the 16 functionals of Table 9 to get CT excitation energies. These five complexes are very different from those used in the LRCTEE9 database (which is part of the training set), which also has CT complexes. The revM11 value of 0.4 for ω is intermediate between that of the "off-the-shelf" γ (= 0.5) and the tuned γ* (= ~0.3) in Tables 1 and 2 of Ref. 53, and the MUE (= 0.38 eV) one gets with revM11 is intermediate between the MUEs obtained with the two γ values when they are used with the range-separated BNL functional[115] in Ref. 53. For the EEAroT5 database, M11 does better than revM11, but revM11 is found to be nearly as good as other range-separated hybrid functionals in Table 9.

The EE69 database has vertical excitation energies for 11 organic molecules – acetaldehyde, acetone, ethylene, formaldehyde, isobutene, pyrazine, pyridazine, pyridine, pyrimidine, *s*-tetrazine, and *s-trans*-butadiene. For each molecule, we look at both valence and Rydberg excitations. Of the total of 69 excitations in the EE69 database, 30 are valence and 39 are Rydberg states. Some of the molecules in EE69 are the same as those used in EE23 but unlike the EE23 database, the EE69 database has higher order excitations for each molecule (not just the lowest-energy excitation). The results in Table 9 show that revM11 not only improves over M11 (MUEs are 0.30 and 0.50 eV, respectively, for revM11 and M11), but it and ωB97X-D are the best range-separated functionals for EE69 in in Table 9.

The EER5 database consists of two vertical excitation energies of 11-*Z-cis*-retinal and three vertical excitation energies of the analogous 11-*Z-cis*-7,8-dihydroretinal compound resulting in a total of five excitations. For 11-*Z-cis*-retinal, the S_1 and S_2 excitations are considered, and for 11-*Z-cis*-7,8-dihydroretinal, the S_1, S_2, and S_3 excitations are considered. The S_3 of dihydroretinal is a $\sigma \rightarrow \pi^*$ excitation, and the remaining four excitations are $\pi \rightarrow \pi^*$ excitations. The revM11 functional overestimates the five excitation energies, especially for the S_1 and S_3 excitations of dihydroretinal, and this yields a large MUE of 0.71 eV for the EER5 database.

The LRCTEE2 database consists of long-range charge transfer excitations of two complexes – the $^3B_2$ state of $C_2F_4\cdots C_2H_4$ at 8 Å and $^3A_1$ state of $NH_3\cdots F_2$ at 6 Å. Neither of these complexes were part of the LRCTEE9 charge transfer subdatabase used for training. The revM11 functional has an MUE of 0.40 eV, which is a significant improvement as compared to M11 (MUE = 0.88 eV). Also, revM11 gives the smallest MUE in Table 9; the second and third best functionals are ωB97 and LC-ωPBE, with MUEs of 0.53 and 0.59 eV, respectively. This trend is similar to what was seen for the LRCTEE9 database in Table 7.

9.1.3 Unified discussion of performance for excitation energies

In this section we combine the performance for excitation energies in the training set of Database 2019 and the additional test data of Database 2019 to obtain a unified assessment on all available excitation energy tests in both the databases. Table 10 summarizes the performance of 16 density functionals that are tested in this work on eight excitation energies databases (two in the training set of Database 2019 and six in the additional test data of Database 2019) that involve LR-TDDFT

calculations. This section highlights the overall performance of each functional on all the valence, all the Rydberg, and all the CT excitations.

Table 10. Mean unsigned errors (in eV) for all valence, all Rydberg, and all CT excitations using 16 density functionals.

Functional	ValEE68[a]	RydEE47[b]	CTEE24[c]	EE139[d]
PBE	0.38	1.36	3.97	1.33
B3LYP	0.23	0.83	2.94	0.90
M06-2X	0.31	0.32	1.39	0.50
revM06	0.28	0.32	1.96	0.58
MN15	0.30	0.31	1.86	0.57
CAM-B3LYP	0.31	0.36	1.49	0.53
HSE06	0.25	0.57	2.91	0.82
LC-ωPBE	0.41	0.38	0.55	0.42
HISS	0.39	0.27	2.39	0.69
ωB97	0.40	0.41	0.53	0.43
ωB97X	0.36	0.32	0.68	0.40
ωB97X-D	0.30	0.35	1.21	0.47
M11	0.35	0.62	0.66	0.49
N12-SX	0.27	0.84	2.98	0.93
MN12-SX	0.39	1.81	2.74	1.27
revM11	0.34	0.31	0.46	0.35

[a]MUE over valence excitations in EE23, EEA11, AEE15, and EE69 databases (= 68 in total).
[b]MUE over Rydberg excitations in EE23, EEA11, and EE69 databases (= 47 in total).
[c]MUE over CT excitations in EE23, EEAroT5, EER5, LRCTEE9, and LRCTEE2 (= 24 in total).
[d]MUE over all the excitation (valence, Rydberg, and CT) (= 139 in total).

The total number of valence excitations tested in this work is 139, obtained by adding 18 valence excitations in EE23, 5 in EEA11, 15 in AEE15, and 30 of EE69. Combining all these tests yields a cumulative database that we will call EE139. Although a few excitations appear in both EE23 and EE69, these tests use different basis sets so trying to eliminate the duplicates in EE139 would involve some arbitrary decisions, and therefore we did not attempt that.

The best functional in Table 10 for the 68 valence excitations is B3LYP, which has an MUE of only 0.23 eV. The other global hybrids (M06-2X, revM06, and MN15) in Table 10 also give reasonable errors, with MUEs ~0.3 eV. Of the 11 range-separated functionals, the best functional is N12-SX with MUE of 0.27 eV, the next best are CAM-B3LYP and ωB97X-D both with MUE 0.30 eV, and after that are M11 and revM11 both with MUE 0.34 eV.

The total number of Rydberg excitations tested in this work is 47, obtained by adding 2 from EE23, 6 from EEA11, and 39 from EE69. The best functional in Table 10 for the 47 Rydberg excitations is HISS, which is a middle-range functional, and the next best functionals are MN15 and revM11 both with MUE of 0.31 eV. The next best functionals, ωB97X, M06-2X and revM06 have MUEs only 0.01 eV larger.

The total number of CT excitations tested in this work is 24, obtained by adding 3 from EE23, 5 from EEAroT5, 5 from EER5, 9 from LRCTEE9, and 2 from LRCTEE2. The best functional in Table 10 for the 24 CT excitations is revM11 with an MUE of 0.46 eV and the second and third best are ωB97 and LC-ωPBE with MUEs 0.53 and 0.55 eV, respectively. Note that, most of the functionals give MUE > 1 eV, including the popular M06-2X and ωB97X-D functionals; this illustrates that predicting CT excitations accurately with DFT is very difficult. High HF exchange is required for CT, especially for long-range CT excitations, and in Table 10 the only functionals that give reasonable value are revM11, LC-ωPBE, ωB97, and ωB97X, which have 100% HF exchange at long range. But these functionals give reasonable CT excitations only at the cost of deteriorating other excitations such as valence, for which high HF exchange can be detrimental, which can be seen from Table 10.

If we compare only the three long-range corrected functionals, revM11, ωB97, and LC-ωPBE, which were the three best for CT excitations, we see that for both valence and Rydberg excitations, ωB97 and LC-ωPBE have MUEs ~0.4 eV, while revM11 has MUE ~0.3 eV. Hence, for all three types of excitations considered independently, revM11 does better than ωB97 and LC-ωPBE in each category.

Overall if we look at all 139 excitations tested in this work using TDDFT, the best functional is revM11 with an MUE of 0.35 eV, the second and third best functionals are ωB97X and LC-ωPBE with MUEs of 0.40 and 0.42 eV, respectively.

Having shown that we achieved our primary objective of obtaining a functional with good results for all three kinds of electronic excitation, we next examine how well we met our second objective of obtaining the best possible ground-state properties consistent with obtaining good excitation energies for all three types of electronic excitation while also keeping the functional smooth with a higher value for the smoothness parameter than used in previous work and with fewer terms than in the M11 functional.

9.2 Performance for ground-state properties

9.2.1 Performance on ground-state properties of subdatabases in Table 2

Single-reference bond energies. The databases SR-MGM-BE8, SR-MGN-BE107, SR-TM-BE15 represent single-reference bond energies of main-group metal, main-group nonmetal, and transition metal containing systems. In Table 7, the revM11 functional improves over M11 for SR-MGM-BE8 and SR-TM-BE15 databases and for SR-MGN-BE107 database its performance compared to M11 is worse by only 0.6 kcal/mol.

Multi-reference bond energies. The databases MR-MGM-BE4, MR-MGN-BE17, and MR-TM-BE12, represent multi-reference bond energies of main-group metal, main-group nonmetal, and transition-metal containing systems. The revM11 functional improves over M11 for these three multi-reference databases. The MR-TMD-BE3 database contains bond energies of three transition-metal dimers (V_2, Cr_2, and Fe_2) all of which are multireference in character and these are more challenging systems than those in other three multi-reference databases. For all four multi-reference databases, revM11 does better than M11 functional and the improvement for the MR-TMD-BE3 database especially deserves attention as the MUE drops by ~35 kcal/mol. Most of the density functionals in Tables 7 and 8 fail catastrophically for the MR-TMD-BE3 database and the ones that do well are local functionals and among local functionals, M06-L is the only functionals that gives an MUE less than 10 kcal/mol. This could be because the dimers of MR-TMD-BE3 database have unique bonding pattern between their atoms and deserve special attention, which is hard to accommodate when fitting a wide variety of data.

Barrier heights. The barrier heights databases used in training the new functional are hydrogen transfer barrier heights (HTBH38/18) of 19 reactions and non-hydrogen transfer barrier heights (NHTBH38/18) of 19 reactions, where both forward and reverse barrier heights are considered for each reaction leading to 38 data for each of these databases. These two databases are sometimes combined and referred to as BH76. The average MUE over HTBH38 and NHTBH38 databases with revM11 is less than 2 kcal/mol, which is not an improvement over M11 but is still reasonable when one considers the improvement on other databases. Tables 7 and 8 show that in general hybrid functionals do much better than local functionals for barrier heights, as one would expect from previous experience.

Noncovalent interaction energies. Three noncovalent interaction energies databases, namely NCCE30/18, NGD21/18, and S6x6 were used in the optimization of the revM11 functional. They are collectively referred to as the NC87 database. On the NCCE30/18 database, revM11 is the

fourth best functional, with an MUE of 0.4 kcal/mol, behind the M11, M06-2X, and ωB97X-D functionals. On the NGD21/18 database it is fourth best functional preceded by ωB97X, MN15-L, and MN15 functionals, and on the S6x6 database it is the third functional and is preceded by MN15, and ωB97X-D, which has damped-dispersion molecular mechanics terms designed to improve its performance for noncovalent interactions.

Ionization potentials, electron affinities, and proton affinities. The ionization potential (IP), electron affinity (EA), and proton affinity (PA) are fundamental quantities for which accurate experimental values are readily available for atoms and small molecules. Therefore, these quantities provide good data for benchmarking and optimizing density functionals. Here we use the IP23, EA13/03, and PA8 databases to optimize the revM11 functional, and in Table 7 we see that for two of them, in particular EA13/03 and PA8, revM11 has an MUE less than 2 kcal/mol, and for IP23, the MUE is 4.0 kcal/mol, which improves quite significantly over the M11 functional, which has an MUE of 7.9 kcal/mol for the IP23 database.

Isomerization energies. There are 14 isomerization energies in the training set (IsoE14), which are divided into three subdatabases: 2pIsoE4, 4pIsoE4, and IsoL6/11. Table 7 shows that the revM11 functional has small MUEs on these databases (< 2.5 kcal/mol), and therefore it is a promising functional for isomerization energies of both large and small molecules.

Other energetic databases. A number of additional energetic databases were used in optimizing the revM11 functional. These are πTC13, AE17, HC7/11, SMAE3/19, DC9/19, and ABDE13, which contain thermochemistry of organic systems containing π bonds, total electronic energies of the first 17 atoms of the periodic table, hydrocarbon chemistry, atomization energies of sulfur molecules, reaction energies of cases that have proven to be difficult for DFT, and alkyl bond dissociation energies of organic molecules, respectively. Our recent work has shown that, with modern density functionals, most of the systems in DC9/19 database do not give especially large errors, and therefore it no longer seems to be a difficult case for DFT. Except for the HC7/11 database, the revM11 functional does reasonably well for the remaining five databases; it gives the second best performance for πTC13 among 23 functionals, being behind the M06-2X functional by only 0.1 kcal/mol.

Geometries of molecules. The MS10 database contains 10 molecular structures divided into two subdatabases – DGL6 and DGH4. The systems in DGH4 provide a different kind of challenge than those in DGL6 because they contain at least one heavy element. In Tables 7 and 8 we can see that

of all the hybrid functionals tested, revM11 and CAM-B3LYP give the smallest MUE (= 0.010 Å) for the DGH4 database. As we shall see in 9.2.2, revM11 is also found to be good for predicting geometries of even more challenging systems than those in the DGH4 database.

The mean unsigned error over the 467 energetic data in AME467 is 2.7 kcal/mol for revM11, which is a significant improvement over M11 that has an MUE of 3.3 kcal/mol. Moreover, of the 11 range-separated hybrid functionals in Table 7, revM11 has the smallest value for this average. Comparing the MUE for AME467 in both Tables 7 and 8, we find that revM11 is the fifth best functional among 23 functionals.

9.2.2 Performance on ground-state properties of subdatabases in Table 3

Barrier heights. Recently[18] we included four barrier heights databases (BHDIV10, BHPERI26, BHROT27, and PX13 – referred to as NewBH76 here) from Ref. 19 (the GMTKN55 database) in Database 2018, and they are also part of the additional test data of Database 2019 to test the performance of various density functionals. Additionally, we test a transition-metal reaction barrier heights database (the TMBH22 database) that has six reactions involving Mo, seven reactions involving W, four reactions involving Zr, and five reactions involving Re. In Table 11 we show the performance of revM11 on all these subdatabases plus the BH76/18 database. Finally we combine all 174 data in these databases into a new composite called BH174, and the MUEs for this composite are shown in the last column.

Table 11. Mean unsigned errors (kcal/mol) on barrier heights databases.

Functional	BHDIV10	BHPERI26	BHROT27	PX13	NewBH76[a]	TMBH22	BH76/18[b]	BH174[c]
BLYP	5.3	4.6	0.4	7.0	3.6	4.4	8.2	5.7
PBE	8.2	3.9	0.5	11.6	4.6	3.5	9.1	6.4
TPSS	6.1	2.2	0.5	8.4	3.2	2.8	8.5	5.5
M06-L	3.1	1.9	1.0	0.9	1.6	2.6	4.1	2.8
revM06-L	2.4	3.9	1.1	6.0	3.1	2.5	2.1	2.6
MN15-L	2.1	1.8	0.9	6.4	2.3	1.9	1.7	2.0
B3LYP	2.8	4.3	0.4	3.6	2.6	3.1	4.5	3.5
PBE0	4.3	1.3	0.6	6.2	2.3	2.3	4.0	3.0
M06	1.9	2.3	0.7	1.5	1.5	1.3	2.3	1.8
M06-2X	1.0	1.4	0.4	5.4	1.7	2.5	1.3	1.6
revM06	1.3	2.3	0.7	1.1	1.4	2.0	1.3	1.4
MN15	1.7	1.3	0.5	2.0	1.2	1.9	1.4	1.4
CAM-B3LYP	1.9	4.6	0.4	4.5	2.8	3.2	3.0	2.9
HSE06	4.2	1.2	0.6	5.8	2.2	2.1	4.1	3.0
LC-ωPBE	1.5	4.8	0.6	4.5	2.8	4.4	1.7	2.5
HISS	1.8	2.3	0.9	2.9	1.8	3.2	1.5	1.8
ωB97	1.8	5.1	0.4	2.0	2.4	3.7	2.1	2.4
ωB97X	1.3	4.4	0.4	1.1	2.0	3.4	2.5	2.4
ωB97X-D	1.2	2.2	0.4	1.5	1.3	2.3	3.2	2.3
M11	1.5	2.2	0.7	3.5	1.8	2.7	1.3	1.7
N12-SX	4.0	1.4	0.9	5.8	2.3	2.7	3.4	2.8
MN12-SX	1.7	2.8	0.6	2.4	1.8	1.8	1.1	1.5
revM11	1.7	3.7	0.5	5.1	2.5	3.3	1.9	2.3

[a]The NewBH76 database includes BHDIV10, BHPERI26, BHROT27, and PX13.

[b]The BH76/18 database includes HTBH38/18 and NHTBH38/18.

[c]The BH174 database is the union of NewBH76, TMBH22, and BH76/18.

The revM11 functional is slightly worse than M11 for all of the databases in table 11 except BHROT27. However, the average MUE on BH174 for the 23 functionals in Table 11 is 2.8 kcal/mol, and the MUE on BH174 for revM11 is only 2.3 kcal/mol.

Geometries. Our training set has geometries for only 10 molecules (MS10 database). The performance of the revM11 functional is tested on three non-training databases involving geometries, which represent a diverse set of systems including systems very different from those used in training the new revM11 functional. These three databases are (a) the MGBL193 database, which has 47 molecules and ions and for each one of them at least one bond distance is considered, resulting in 193 bond lengths, (b) the TSG48 database, which has transition-state (TS) geometries for 16 reactions and for each of the 16 TS structures, three bond distances are considered, which results in a total of 48 bond lengths in the TSG48 database, and (c) the TMDBL10 database, which has 10 transition-metal dimers, and hence 10 bond lengths. The results for the three databases are shown in Table 12. The 16 TS structures of the TSG48 database are characterized by the presence of one imaginary frequency for each density functional reported in Table 12. For the TMDBL10 database, the results were quite different with and without the stability check for some of the dimers, and in Table 12 the values for the most stable solution are given.

For the MGBL193 database, most of the density functionals do well and have MUEs less than 0.010 Å with the exceptions being the local functionals, BLYP, PBE, and MN15-L, which have MUEs ≥ 0.010 Å. The M11 and revM11 functionals give the same MUE to the number of decimal places reported in Table 12 and are comparable in performance to the other hybrid functionals in the table. As one goes from the MGBL193 database to the TMDBL10 database, the errors in bond lengths increase for each density functional, as one would expect for these difficult dimers, which can be inherently multiconfigurational in nature. In general, the local functionals have smaller MUEs than the hybrid functionals, which could be due to the fact that, in hybrid density functionals, HF exchange causes static correlation error. In any case, the revM11 functional (MUE = 0.078 Å) improves quite significantly over the M11 (MUE = 0.104 Å) functional for the TMDBL10 database. In contrast to the TMDBL10 database, for the TSG48 database in Table 12, the hybrid functionals in general do better than the local functionals and revM11 is the third best performing functional (MUE = 0.019 Å) of the 23 functionals, and is behind M06-2X, and LC-ωPBE by only 0.002 and 0.001 Å, respectively.

Table 12. Mean unsigned errors (Å) on databases with geometries.

Functional	MGBL193[a]	TSG48	TMDBL10	MS10
BLYP	0.012	0.123	0.061	0.027
PBE	0.010	[0.141][b]	0.043	0.016
TPSS	0.008	0.112	0.058	0.012
M06-L	0.004	0.057	0.059	0.007
revM06-L	0.008	0.052	0.069	0.009
MN15-L	0.010	0.043	0.061	0.012
B3LYP	0.004	0.065	0.084	0.017
PBE0	0.005	0.036	0.083	0.008
M06	0.006	0.037	0.073	0.012
M06-2X	0.004	0.017	0.163	0.022
revM06	0.005	0.029	0.094	0.012
MN15	0.003	0.021	0.070	0.007
CAM-B3LYP	0.004	0.032	0.075	0.009
HSE06	0.005	0.038	0.082	0.008
LC-ωPBE	0.006	0.018	0.068	0.012
HISS	0.008	0.024	0.094	0.012
ωB97	0.005	0.022	0.076	0.014
ωB97X	0.004	0.025	0.082	0.012
ωB97X-D	0.004	0.030	0.083	0.012
M11	0.006	0.020	0.104	0.011
N12-SX	0.006	0.035	0.089	0.007
MN12-SX	0.007	0.023	0.077	0.009
revM11	0.006	0.019	0.078	0.010

[a]This database developed by Piccardo *et al.*[69] has a set of 47 semi-experimental equilibrium structures. We called it SE47 in our recent work;[16] it has been renamed here and comprises 193 bond lengths of 47 molecules and ions.

[b]The MUE for the PBE functional is obtained by averaging over 14 transition structures (42 bond lengths), excluding reactions R1 and R6. Reactions R1 and R6 were excluded because the transition structure could not be located for these reactions with this functional. See Table S47 of the Supporting Information.

Self-interaction error and delocalization error. One of the major sources of error in KS-DFT is self-interaction error (SIE). Adding HF exchange to a local density functional mitigates SIE to some extent but the effect of SIE can be very pronounced for the interaction of charged fragments. Here the SIE4x4 database is used as a test for self-interaction error of the 23 density functionals tested in this work. The SIE4x4 database has four doublet cation complexes (H_2^+, He_2^+, $(NH_3)_2^+$, and $(H_2O)_2^+$) with each complex at four intermonomer distances (1.0, 1.25, 1.5,

and 1.75 times the equilibrium intermonomer distance). The results for the SIE4x4 database are presented in Table 13.

For delocalization error test, we consider the stretched NaCl molecule with 10 Å separation between Na and Cl atoms. Table 13 also present results for the ability of the 23 tested density functionals to predict charges on Na and Cl atoms at 10 Å. At 10 Å, the system should already be separated into neutral atomic fragments, so any partial charge on the fragments (either a whole charge or a partial charge) at this distance is an error and in particular is a measure of charge delocalization error. The choice of 10 Å distance between Na and Cl atoms is arbitrary, but large enough for a consistent comparison of density functionals. Table 13 shows the charge on Na at 10 Å in spin-unrestricted calculations.

Table 13. Mean unsigned errors (kcal/mol) on SIE4x4 database and charge q (in atomic units) on Na atom of NaCl at 10 Å separation between Na and Cl atoms.

Functional	**SIE4x4**[a]	q**(Na)**[b]
BLYP	24.7	0.454
PBE	23.4	0.462
TPSS	21.5	0.473
M06-L	17.9	0.614
revM06-L	14.2	0.502
MN15-L	11.0	0.517
B3LYP	17.6	0.445
PBE0	14.1	0.445
M06	14.2	0.535[c]
M06-2X	8.6	0.421
revM06	11.3	0.485
MN15	11.3	0.482
CAM-B3LYP	13.5	0.400
HSE06	14.3	0.449
LC-ωPBE	9.4	0.000
HISS	8.6	0.445
ωB97	10.4	0.995
ωB97X	11.4	0.995
ωB97X-D	13.4	0.536
M11	9.6	0.908
N12-SX	14.4	0.500
MN12-SX	9.0	0.538
revM11	10.6	0.000

[a]The self-interaction error energy is calculated as the difference in energies between the complex and the monomers infinitely separated from each other.

[b]The charge on Na atom is calculated from the dipole moment of NaCl at 10 Å separation between Na and Cl atoms. Note that the charges obtained with some of the functionals presented in this table were also presented in Table 1 of Ref. 116.
[c]This datum is calculated with the aug-cc-pV(T+d)Z basis set, while charges using other density functionals are calculated with the basis set mentioned in Table 5.

Local density functionals are expected to yield large errors for SIE4x4, and three (PBE, BLYP, and TPSS) of the six local functionals (PBE, BLYP, TPSS, M06-L, revM06-L, and MN15-L) give MUEs greater than 20 kcal/mol. The best local functional is MN15-L (MUE = 11.0 kcal/mol), and its errors are comparable to some of the hybrid density functionals in performance. The M11 and revM11 give similar MUEs for the SIE4x4 database and are within 1 kcal/mol of each other.

In delocalization error test, we found that only two of the 23 functionals give zero charge on Na atom; both these functionals, LC-ωPBE and revM11, are long-range corrected functionals which have 100% HF exchange at large interelectronic separations. Additionally, we found in a recent work (Table 1 of Ref. 116) that functionals such as HFLYP, M06-HF, and LC-BLYP, which have 100% HF exchange at large interelectronic separations also give zero charge on Na at 10 Å. It is perhaps surprising though that four long-range corrected functionals (M11, ωB97, ωB97X, and ωB97X-D) in Table 13 do not yield zero charge on Na atom at 10 Å, although going beyond 10 Å will result in zero charge with these functionals. An important point to be noted here is that revM11 improves significantly over M11 in predicting the charge.

Dipole moments. In a recent work,[66] dipole moments of 78 molecules (DM78 database) representing a diverse set of molecules were reported using 48 density functionals. These 78 molecules were divided into single-reference (SR) and multi-reference (MR) molecules based on B_1 diagnostics,[20] of which 55 were found to be single reference and 23 were found to be multireference. Here we add one more molecule, NaLi, to the set of 78 molecules, giving rise to the DM79 database. The NaLi molecule is found to be single reference, which increases the count of single-reference molecules to 56. The dipole moment is the first moment of the charge distribution, and as such it is a key measure of the accuracy of electron densities.

Each molecule is consistently optimized with each density functional; that is, each calculated dipole moment is at a different geometry, namely the one predicted by the functional being tested. The results are presented in Table 14, where we see that 19 of the 23 functionals give MUEs on 79 molecules in the range 0.21—0.30 D. The 23 multi-reference molecules distinguish

the performance of the functionals more than do the 56 single-reference molecules, and the range of MUEs for multi-reference molecules is very wide – from 0.35 D to 0.79 D. In contrast, the range of MUEs for single-reference molecules is only 0.14–0.27 D. The revM11 functional improves over M11 for both SR and MR molecules and its MUE over all the 79 molecules is 0.30 D. Note that the dipole moment is not in the training set of revM11 optimization.

Table 14. Mean unsigned errors (in Debye) on the DM79 database.[a]

Functional	**SRDM56**[b]	**MRDM23**[c]	**DM79**[d]
BLYP	0.19	0.39	0.25
PBE	0.18	0.40	0.24
TPSS	0.16	0.39	0.22
M06-L[e]	0.20	0.36	0.24
revM06-L	0.20	0.35	0.25[e]
MN15-L	0.21	0.40	0.26
B3LYP	0.16	0.39	0.22
PBE0	0.14	0.36	0.21
M06	0.15	0.43	0.23
M06-2X	0.21	0.58	0.32
revM06	0.17	0.43	0.24
MN15	0.16	0.51	0.27
CAM-B3LYP	0.17	0.52	0.27
HSE06	0.14	0.36	0.21
LC-ωPBE	0.20	0.54	0.30
HISS	0.17	0.59	0.30
ωB97	0.19	0.61	0.31
ωB97X	0.19	0.52	0.28
ωB97X-D	0.17	0.48	0.26
M11	0.27	0.68	0.39
N12-SX	0.17	0.46	0.25
MN12-SX	0.18	0.79	0.36
revM11	0.17	0.62	0.30

[a]Some of the results in this table were also presented in Ref. 66.

[b]MUE over dipole moments of 56 single-reference molecules

[c]MUE over dipole moments of 23 multi-reference molecules

[d]MUE over dipole moments of all the 79 molecules

[e]MUE (DM79) is smaller for M06-L than for revM06-L by 0.01 D, which seems incongruous given that MUE (SRDM56) is shown to be the same for M06-L as for revM06-L and MUE (MRDM23) for M06-L is shown to be 0.01 D higher than that of revM06-L. However, the numbers are correct, and the seeming inconsistency is simply a result of rounding all values in the table to two decimal places.

Noncovalent interaction energies. The noncovalent interaction energies are tested for two databases, which consist of noncovalently bound systems, the S66x8 and PEC4 databases.

The S66x8 database and its subdatabases were designed with the objective of validating quantum mechanical methods.[34] The S66x8 database contains interaction energies of 66 complexes relevant to biomolecular structures at 8 interacting distances for each – 0.90, 0.95, 1.00, 1.05, 1.10, 1.25, 1.50, and 2.00 times the equilibrium distance. Table 15 gives MUEs for the S66x8 database, its subset S66, and three subsets of S66. The S66 database has interaction energies of the 66 complexes at their equilibrium distances, and it is further subdivided into DD23, HB23, and Mix20 subdatabases, which correspond subdatabases respectively to dispersion-dominated complexes, hydrogen-bonding dominated complexes, and complexes that are dominated by a mix of damped dispersion and electrostatics. Note that, the S6x6 database, which is a different subset of the S66x8 database, contains six of the complexes (water…peptide, uracil…uracil, and acetic acid…acetic acid from HB23, benzene…uracil and pyridine…uracil from DD23, and benzene…benzene (T-shaped CH…π interaction) from Mix20) at six interacting distances each (0.90, 0.95, 1.00, 1.05, 1.10, and 1.25 times the equilibrium distance), and it was used in training the revM11 functional.

Table 15. Mean unsigned errors (kcal/mol) for the S66x8 database, its subdatabase S66, and three subdatabase (DD23, HB23, and Mix20) of S66.

Functional	**DD23**[a]	**HB23**[a]	**Mix20**[a]	**S66**[b,c]	**S66x8**[c,d]	**S492**[e]	**S462**[f]
BLYP	6.19	2.15	3.69	4.02	2.95	2.87	2.80
PBE	3.64	0.71	1.89	2.09	1.50	1.46	1.42
TPSS	4.83	1.34	2.69	2.97	2.10	2.04	1.98
M06-L	0.60	0.38	0.72	0.56	0.46	0.45	0.45
revM06-L	0.41	0.51	0.48	0.47	0.45	0.45	0.45
MN15-L	2.43	1.36	1.00	1.62	1.06	1.02	0.98
B3LYP	5.15	1.38	2.91	3.16	2.32	2.26	2.20
PBE0	3.58	0.63	1.79	2.01	1.45	1.41	1.37
M06	0.83	0.43	0.72	0.65	0.56	0.55	0.55
M06-2X	0.30	0.22	0.26	0.26	0.29	0.29	0.29
revM06	0.24	0.29	0.26	0.26	0.26	0.26	0.26
MN15	0.57	0.36	0.32	0.42	0.32	0.31	0.31
CAM-B3LYP	3.77	0.54	1.95	2.09	1.55	1.51	1.47
HSE06	3.51	0.54	1.73	1.94	1.39	1.35	1.31
LC-ωPBE	3.84	1.32	2.09	2.43	1.76	1.71	1.66
HISS	3.24	0.48	1.51	1.75	1.27	1.23	1.20
ωB97	0.29	0.56	0.20	0.35	0.42	0.43	0.43

ωB97X	0.74	0.48	0.36	0.53	0.52	0.52	0.52
ωB97X-D	0.47	0.28	0.21	0.32	0.23	0.22	0.22
M11	0.62	0.40	0.36	0.47	0.43	0.43	0.42
N12-SX	3.67	0.56	1.88	2.04	1.59	1.56	1.53
MN12-SX	1.03	1.02	0.80	0.96	0.85	0.84	0.83
revM11	0.30	0.38	0.33	0.34	0.30	0.30	0.29

[a]DD23, HB23, and Mix20 are the three subdatabases of the S66 database and correspond to dispersion dominated, hydrogen bonding, and mixed subdatabases, respectively.

[b]S66 contains interaction energies of 66 non-covalently bound complexes at their equilibrium distance.

[c]Note that S6x6 contains six data that are also in S66 and S66x8 and in one or another of DD23, HB23, and Mix20, but we present the results for DD23, H23, Mix20, S66, and S66x8 for easy comparisons to other results in the literature.

[d]S66x8 has 66 complexes at 8 interacting distances – 0.90, 0.95, 1.00, 1.05, 1.10, 1.25, 1.50, and 2.00 times the equilibrium distance.

[e]S492 is the complement to S6x6 in S66x8. There is no duplication between S6x6 and S492.

[f]S462 is the complement to S66 in S66x8. There is no duplication between S66 and S462.

We look first at the 22 functionals that do not have molecular-mechanics damped-dispersion terms, and we find that the best performing functional for both S66x8 and its subset S66 is revM06. The revM11 functional improves over M11 for both these databases and its MUE is quite close to revM06 for both of them. The ωB97X-D functional has molecular mechanics dispersion terms and it does well for S66x8, but only slightly better than revM06, M06-2X, and revM11. However, one expects functionals with local correlation and no molecular mechanics to do better for noncovalent complexes at their equilibrium geometries than at long range, and M06-2X and revM06 do significantly better than ωB97X-D at equilibrium geometries (i.e., for the noncovalent binding energies of S66 rather than for the whole potential energy curves of S66x8), and revM11 has an MUE only 0.02 kcal/mol higher than ωB97X-D for S66. We prefer to get noncovalent binding energies without using molecular mechanics, and Table 14 shows good success for this.

The PEC4 database has potential energy curves (PECs) of four inert gas dimers (Ar_2, Kr_2, KrHe, and Ne_2), and for each dimer at least 30 points on the PEC are calculated. Some inert gas dimers, which are part of the NGD21/18 database where equilibrium distances and two distances on either side of the equilibrium distance are considered, were used in training the new functional. But here we test the performance on non-equilibrium distances that go much farther

from the equilibrium distance. Figures 1a, 1b, 1c, and 1d compare the reference potential curves for four rare gas dimers to the results for five density functionals – M11, revM11, M06, M06-2X, and revM06. The display of the M11 and revM11 curves allows us to compare the new functional, revM11, with its parent, M11, and the display of revM06 curves allows us to compare to results for the recent revM06 functional, which has a percentage of HF exchange intermediate between that of M06 and that of M06-2X. The M06-2X functional is known to usually provide reasonably good accuracy for noncovalent interaction energies, and we want to see how well the recent functionals, revM11 and revM06, perform in comparison to it. In Figure 1, the revM11 curves are little bit smoother than the M11 curves. For all four inert gas dimers shown in these figures, revM11 gives tighter binding than experiments at short interatomic distances and gives a binding energy similar to experiments at medium-to-long interatomic distances.

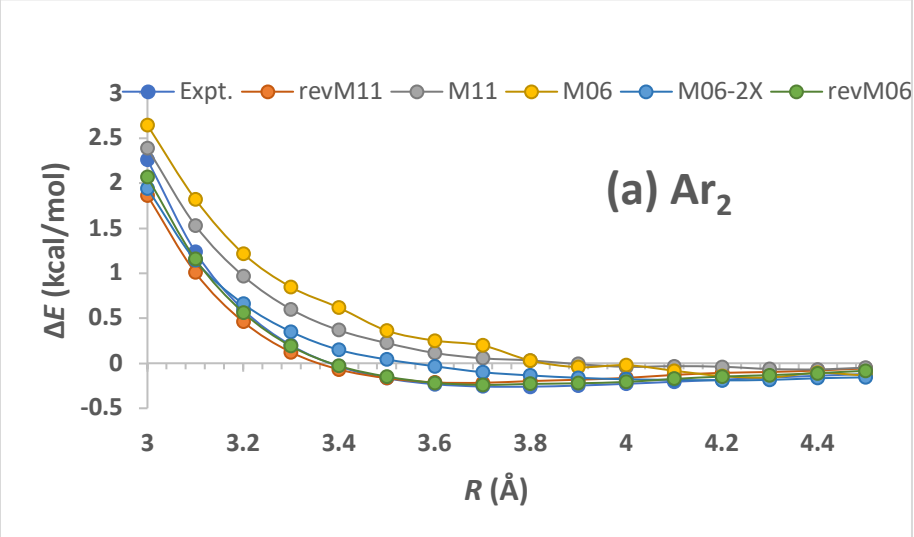

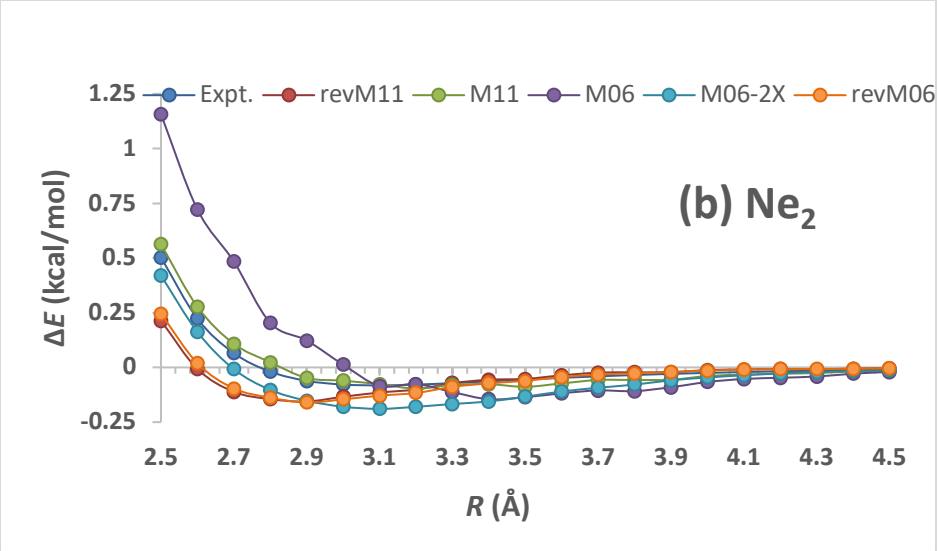
Expt.
revM11
M11
M06
M06-2X
revM06
(b) Ne2
ΔE (kcal/mol)
R (Å)
1.25
1
0.75
0.5
0.25
0
-0.25
2.5
2.7
2.9
3.1
3.3
3.5
3.7
3.9
4.1
4.3
4.5

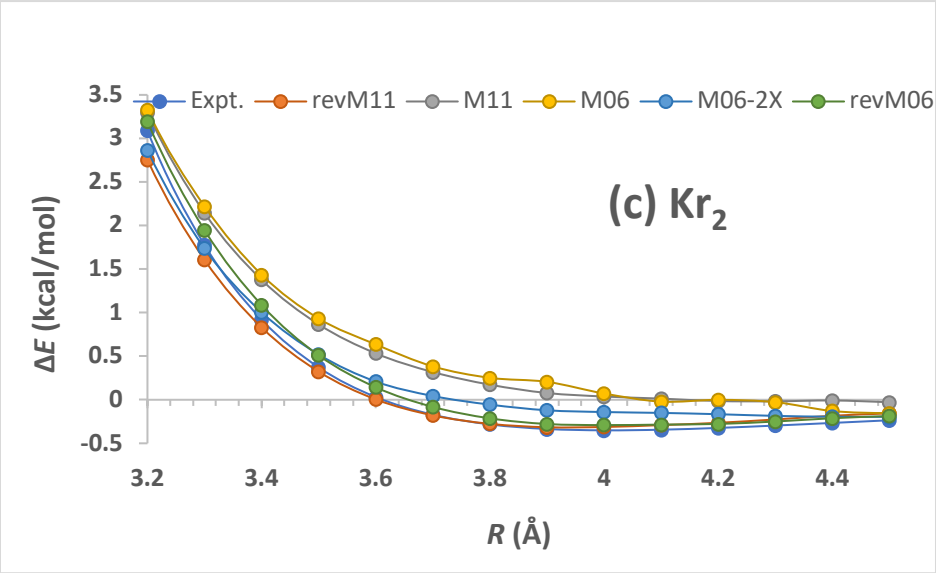
Expt.
revM11
M11
M06
M06-2X
revM06
(c) Kr2
ΔE (kcal/mol)
R (Å)
3.5
3
2.5
2
1.5
1
0.5
0
-0.5
3.2
3.4
3.6
3.8
4
4.2
4.4

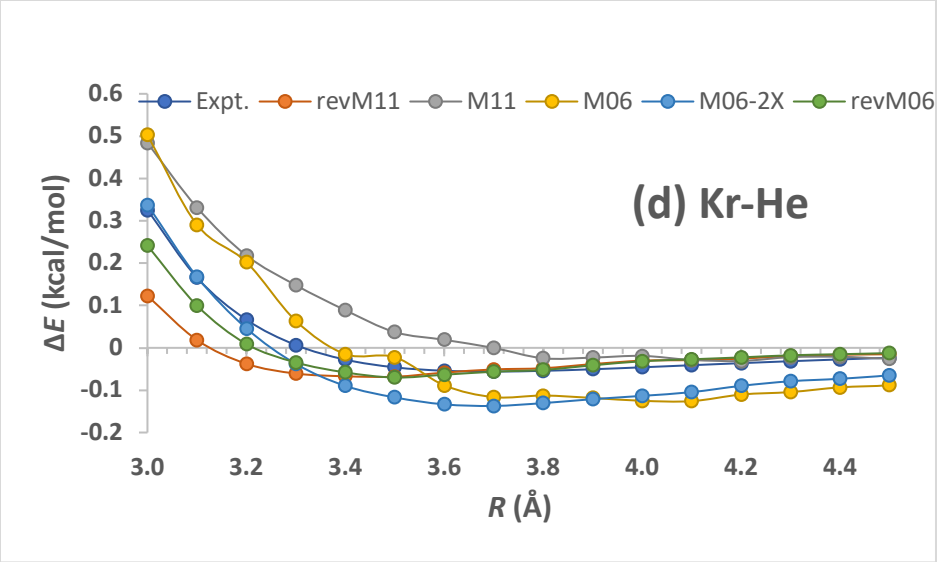

Figure 1. Potential energy curves of (a) Ar_2, (b) Ne_2, (c) Kr_2, and (d) KrHe calculated using M11, revM11, M06, M06-2X, and revM06 density functionals with the aug-cc-pVQZ basis set.

Other subdatabases of the additional test data of Database 2019. The other databases in the additional test data of Database 2019 include Al2X6, DIPCS10, HeavySB11, YBDE18, WCCR10, and ASNC2, where the Al2X6, DIPCS10, HeavySB11, and YBDE18 databases are taken from the GMTKN55 database.[19] The mean unsigned errors for these databases are reported in Table 16 for revM11 and 22 other density functionals.

Table 16. Mean unsigned errors (kcal/mol) on other subdatabases of Table 3.

Functional	Al2X6	DIPCS10	HeavySB11	YBDE18	WCCR10	ASNC2
BLYP	12.0	7.9	8.1	11.1	9.8	7.7
PBE	4.3	4.6	4.6	5.9	6.8	2.7
TPSS	4.0	3.8	4.5	7.3	7.1	3.6
M06-L	0.8	8.4	2.7	4.9	5.9	3.4
revM06-L	1.5	9.5	2.7	5.5	5.4	6.4
MN15-L	1.4	10.3	6.5	4.2	6.4	7.6
B3LYP	8.9	4.4	7.6	8.2	7.6	4.7
PBE0	2.8	2.9	3.6	2.5	5.8	1.6
M06	3.0	6.5	1.9	4.9	5.3	2.4
M06-2X	0.9	3.1	8.3	2.5	6.0	1.2
revM06	0.9	2.7	2.2	3.0	5.4	2.2
MN15	1.5	4.3	5.1	3.4	7.5	1.6
CAM-B3LYP	6.0	4.3	7.3	5.4	5.5	0.5
HSE06	3.0	3.1	3.2	3.0	5.6	1.0
LC-ωPBE	2.3	3.0	6.6	2.9	5.9	2.2

HISS	1.9	4.0	4.2	3.1	5.5	1.0
ωB97	2.7	5.4	3.5	1.4	7.6	1.2
ωB97X	3.3	5.6	3.1	2.1	7.0	1.0
ωB97X-D	3.1	5.4	2.2	2.8	8.5	0.5
M11	1.3	3.3	2.0	1.8	6.2	2.8
N12-SX	2.5	5.7	2.9	2.4	6.6	0.9
MN12-SX	3.2	8.2	1.9	3.9	4.9	3.2
revM11	0.6	4.9	4.2	2.1	7.0	1.3

The Al2X6 database contains dimerization energies of aluminum compounds. The dimerization energies of six aluminum compounds (Al_2Cl_6, Al_2F_6, Al_2H_6, Al_2Me_4, Al_2Me_5, and Al_2Me_6) were calculated. (Here Al_2Me_5 is a dimer of $AlMe_2$ and $AlMe_3$). The MUEs over the Al2X6 database show that the best performing functional among 23 functionals in Table 16 is revM11 (MUE = 0.55 kcal/mol), which improves considerably over the M11 functional (MUE = 1.32 kcal/mol).

The DIPCS10 database represents double-ionization potentials of 10 closed-shell systems, which include both organic and inorganic systems. The systems are Be, C_2H_4, C_2H_6, C_4H_4, CH_2O, H_2S, Mg, N_2H_2, NH_3, and PH_3. The MUE over this database for the revM11 functional is 4.9 kcal/mol. Even though it does not do better than M11, which has an MUE of 3.3 kcal/mol, it does better than other range-separated hybrid functionals such as ωB97, ωB97X, and ωB97-D, all three of which have an MUE in the range 5.4–5.6 kcal/mol.

The HeavySB11 database has homolytic dissociation energies of 11 covalently bonded dimers where at least one of the monomers involves a “heavy” element (defined for this database as having an atomic number in the range 15 to 82). The dimers are As_2Me_4, Br_2, Cl_2, Ge_2H_6, H_2S_2, P_2Me_4, Sb_2Me_4, Sn_2Me_6, Te_2Me_2, H_2Se_2, and Pb_2Me_6 and they dissociate to give the respective monomer. The revM11 functional has an MUE of 4.2 kcal/mol, only slightly better than the average MUE of all 23 functionals, which is 4.3 kcal/mol.

The YBDE18 database represents ylide bond-dissociation energy of 18 species. This database for benchmarking density functionals was introduced in Ref. 58, and its reference values were updated in Ref. 19 by Grimme and coworkers. The revM11 functional gives an MUE of 2.1 kcal/mol, and it is the third best functional of the 11 range-separated hybrid functionals in Table 16. It is also much lower than the average MUE of all 23 functionals, which is 4.1 kcal/mol.

The WCCR10 database contains reaction energies of 10 reactions, where one of the elements involved in each reaction is a transition metal (Cu, Ag, Au, Pd, Pt, or Ru). In our past work[18] we reported results for the subset WCCR9 of the WCCR10 database because one of the reactions, reaction 4, of this database was found to be computationally very expensive for some of the hybrid functionals. In this work, we loosened the convergence criterion for SCF energy calculations for reaction 4 from 10^{-8} to 10^{-7} or 10^{-6} hartrees, and in Table 16 we report results for the entire WCCR10 database. The MUE with revM11 is 7.0 kcal/mol, which is slightly worse than the average MUE of all 23 functionals, which is 6.5 kcal/mol.

The ASNC2 database contains binding energies of sulfur-nitrogen clusters that are relevant to atmospheric chemistry. It has two complexes (1A1D and 2A1N),[64] where A, D, and N are the monomers of these complexes – A stands for the acid H_2SO_4, D stands for dimethylamine, and N stands for ammonia. The number with each monomer indicates its stoichiometry in the complex. Table 16 shows that the local functionals do better than hybrid functionals for the ASNC2 database, and among hybrid functionals, the range-separated hybrids give the smallest MUE, for example, CAM-B3LYP and ωB97X-D give MUEs of only 0.5 kcal/mol. The revM11 functional has an MUE of 1.3 kcal/mol, which is 0.8 kcal/mol higher than the two best functionals in Table 16 but 1.3 kcal/mol lower than the average MUE of all 23 functionals, which is 2.6 kcal/mol.

10. An attempt at a comprehensive ranking

There is no unambiguous way to assess overall performance of density functionals. The MUE for the cumulative subdatabase AME467 is interesting, but as an overall summary it has two major deficiencies: (i) the data in some of the databases (e.g. IP23) have much larger values than the data in some others (e.g., noncovalent binding energy databases), which give each datum in the former databases a higher relative weight; (ii) the different databases have different numbers of elements, which gives the larger databases more influence in AME467. The MUE for EE139 does not suffer as much from these faults (and therefore it is very encouraging that revM11 has the lowest MUE for EE139), but it still does not reflect our goal of obtaining a functional with good performance in four categories of excitation: valence, Rydberg, long-range charge transfer, and short- and medium-range charge transfer.

For these reasons we prefer another measure, namely average rank. To obtain the average rank, we rank the functionals by MUE on each database; the rank is 1 for the lowest MUE, 2 for

the second lowest, etc.), and then we average these ranks. A low average rank indicates good universality. This clearly eliminates deficiencies i and ii, and it reflects reasonably well our goal of obtaining a functional with good accuracy across the board, although of course it is not perfect (since, as just one example, the number of databases of each type is somewhat arbitrary).

If more than one functional has the same MUE for a given database (to the number of digits shown in the tables), the average rank is returned. For example, if two functional are tied for rank 2, they are each assigned rank 2.5.

First consider ground-state properties. For all of the ground-state databases we have tests for 23 functionals. For ground-state energetics we average the rank over 46 databases, in particular the 24 ground-state energetic databases of Table 2and the 13 ground-state energetic databases of Table 3 (except that – for convenience – we use S462 rather than S432) plus DD23, HB23, and Mix20. For ground-state bond distances we average the ranks over five databases, in particular the two ground-state bond-distance databases of Table 2 and the three ground-state bond-distance databases of Table 3. (It would be redundant to also include MS10 because it is the union of DGL6 and DGH4, which are in Table 2.) The average ranks of the 23 tested functionals are provided in Table 17; the last column of the table is the average of the two average ranks.

Table 17. Average ranks (out of 23 functionals) for energetic databases and bond-distance databases.

Functional	Energies[a]	Bond distances[b]	Average[c]
MN15	6.2	5.3	5.7
revM11	8.9	9.9	9.4
revM06	5.6	13.5	9.6
M06-2X	8.0	11.2	9.6
M06-L	12.7	7.5	10.1
MN12-SX	10.2	10.1	10.2
ωB97X-D	8.8	11.6	10.2
ωB97X	10.2	10.7	10.5
M06	9.5	13.1	11.3
M11	9.8	13.1	11.5
PBE0	13.1	10.2	11.6
CAM-B3LYP	14.7	8.6	11.6
ωB97	11.0	12.5	11.8
HSE06	13.1	10.6	11.9
revM06-L	12.1	12.3	12.2
LC-ωPBE	14.4	10.1	12.3

MN15-L	11.1	13.5	12.3
N12-SX	13.0	11.7	12.3
HISS	13.0	15	14.0
TPSS	16.8	13.9	15.4
B3LYP	17.2	15.9	16.6
PBE	16.9	16.8	16.8
BLYP	19.8	18.9	19.3

[a] Average over 40 databases

[b] Average over 5 databases

[c] Average of previous two columns

We find that revM11 has a rank of 6 or better (out of 23 functionals) on 16 of the 45 databases and a rank of 11 or better on 30 of them. The results in Table 17 are very encouraging; when averaged over both ground-state energetics and ground-state bond distances, revM11 has the second-best average rank.

Consider next the electronic excitation energies. One wants good performance for valence, Rydberg, and charge transfer excitations even if one is nominally interested only in valence excitations. The reason for this is that functionals that do poorly for Rydberg states typically underestimate their excitation energies so the Rydberg states mix in an unphysical way with lower-energy valence states, making the valence states less accurate; furthermore, in complex molecules, various states that are nominally classed as valence states may have different amounts of charge transfer character, and their relative energies can be skewed if the charge transfer character is not treated well. Therefore we average ranks over the three classes of excitation in Table 10. These ranks are in Table 18 in the column marked excitation energies. Table 10 has 16 functionals and Table 18 has those 16 functionals.

Table 18. Average ranks (out of 16 functionals) for ground-state properties and excitation energies.

	Ground state		**Excitation**	
Functional	**Energies**[a]	**Bond distances**[b]	**energies**[c]	**Average**[d]
MN15	5.0	3.5	5.8	4.8
revM11	6.9	6.9	4.3	6.0
M06-2X	6.0	8.0	6.7	6.9
revM06	4.5	10.2	6.3	7.0
ωB97X-D	6.7	8.8	6.3	7.3
ωB97X	7.8	7.8	7.0	7.5

CAM-B3LYP	10.9	6.1	7.3	8.1
M11	7.4	9.6	8.5	8.5
ωB97	8.4	9.0	8.7	8.7
HSE06	9.8	7.8	8.7	8.8
LC-ωPBE	10.7	7.2	8.7	8.9
HISS	9.6	11.1	8.0	9.6
N12-SX	9.7	9.0	10.7	9.8
MN12-SX	7.9	7.4	14.7	10.0
B3LYP	12.5	11.3	9.3	11.1
PBE	12.2	12.3	15.0	13.2

[a] Average over 40 databases

[b] Average over 5 databases

[c] Average over three kinds of excitation in Table 12

[d] Average of previous three columns

The rank of revM11 on the ValEE68, RydEE47, and CTEE24 databases of Table 10 is respectively 8.5, 2.5, and 1, for an average rank of 4.0 (out of 16 functionals). This is the best average rank by a considerable margin; it is followed by 5.5 for MN15, 6.0 for revM06 and ωB97X-D, and 6.3 for M06-2X. This analysis does not separate short-range and long-range charge transfer, so it is also important to note the very good performance of revM11 for LRCTEE9 and LRCTEE2, which contain long-range charge transfers. The good average rank of revM11 combined with its good performance for long-range charge transfer makes a very promising choice for electronic excitation calculations.

Table 18 also shows the result of combining the two ground-state averages ranks with the excitation energy rank; again revM11 ranks very high.

11. Other strategies of optimizing density functionals

The approach taken here is only one route to try to obtain improved functionals. Some other routes may be considered as well. For example, (i) we have considered enhancing exchange at large reduced gradient of density to improve the asymptotic form of the local potential for Rydberg states;[117] (ii) we have considered translating spin-polarized GGAs into functionals of the total density and on-top pair density for use with multiconfiguration wave functions as reference functions to improve the description of strongly correlated systems and excitation energies;[118] (iii) we have considered increasing the local exchange globally as a way to, for example, improve band gaps of semiconductors and some molecular excited states while keeping

the computational cost affordable in plane wave codes,[56,119] and (iv) Kaupp, Janesko, and coworkers have made progress in using local hybids[7] and functionals with rung-3.5 ingredients.[120,121] These approaches involve only a few parameters or even no new parameters, but they could be combined with flexible functional forms such as used here to perhaps further improve the accuracy in future work. The above list is just a sampling of possible routes to further improvement. We anticipate that the quest for higher accuracy and more universal functionals will involve various combinations of improved functional forms, more diverse training databases, and improved reference functions.

12. Concluding remarks

This paper presents the revM11 functional, which is obtained by re-optimizing the M11 range-separated functional. The strategy for optimizing the new functional is to obtain a balanced treatment for electronic excitation energies (simultaneously good performance for all types of excitation energies – valence, Rydberg, short-range charge transfer, and long-range charge transfer) and – with this as a constraint – obtain the best possible performance across a diverse set of databases for ground-state properties. The performance of the revM11 functional was then compared to a variety of density functionals, including ten previous range-separated hybrid density functionals tested on a variety of atomic and molecular properties for ground and excited states.

For excitation energies, we looked at all the three types of excitations, in particular, 68 valence excitations, 47 Rydberg excitations, and 24 charge transfer excitations. The newly optimized revM11 functional has performance similar to M11 for valence excitations (both have an MUE of 0.34 eV), and it improves significantly over M11 for Rydberg and charge transfer states. Although an MUE of 0.34 eV for valence excitations is moderately successful, several other functionals, especially the B3LYP global hybrid, do even better for valence excitations, but revM11 improves significantly over all global hybrids for charge transfer excitations, and it improves significantly over B3LYP for Rydberg excitations. In comparison to ten other range-separated hybrid functionals, revM11 performance similar to most of them for valence excitations, does much better than screened-exchange functionals, HSE06, N12-SX, and MN12-SX, for Rydberg excitations, and is the best for CT excitations. Overall, we find that for 139

TDDFT excitations considered in this work, revM11 with an MUE of 0.35 eV is the best among all the 16 density functionals tested for excitation energies.

For ground-state properties, the revM11 functional improves over the M11 functional for about half of the database; it is significantly better for bond energies involving metal atoms, ionization potentials, and noncovalent interaction energies and significantly less accurate for isomerization energies of large molecules. However, it has relatively good performance across the whole range of databases, and it joins M06-2X, MN15, and revM06 in the class of most universal density functionals devised so far.

■ ASSOCIATED CONTENT

Supporting Information.

The Supporting Information is available free of charge on the ACS Publications website at DOI: 10.1021/

Reference values and calculated values using PBE, B3LYP, M11, and revM11 for each database. (PDF)

■ AUTHOR INFORMATION

Corresponding Authors

*E-mail: verma045@umn.edu (P.V.), xiaohe@phy.ecnu.edu.cn (X.H.), truhlar@umn.edu (D.G.T.)

ORCID

Pragya Verma: 0000-0002-5722-0894
Ying Wang: 0000-0002-4359-3753
Soumen Ghosh: 0000-0003-0850-4855
Xiao He: 0000-0002-4199-8175
Donald G. Truhlar: 0000-0002-7742-7294

Notes

The authors declare no competing financial interest.

■ ACKNOWLEDGMENTS

This work was supported by the Nanoporous Materials Genome Center, which is funded by the U.S. Department of Energy, Office of Basic Energy Sciences, Division of Chemical Sciences, Geosciences and Biosciences under Award DE-FG02-17ER16362. This work was also supported by the National Key R&D Program of China (Grant No. 2016YFA0501700), National Natural Science Foundation of China (Grant Nos. 21673074 and 21761132022), Shanghai Municipal Natural Science Foundation (Grant No. 18ZR1412600), Young Top-Notch Talent Support Program of Shanghai, and NYU-ECNU Center for Computational Chemistry at NYU Shanghai.

We also thank the Supercomputer Center of East China Normal University for providing us computational time.

■ REFERENCES

1. Kohn, W.; Sham, L. J., Self-Consistent Equations Including Exchange and Correlation Effects. *Phys. Rev.* **1965**, *140*, A1133-A1138.

2. Ghosh, S.; Verma, P.; Cramer, C. J.; Gagliardi, L.; Truhlar, D. G. Combining Wave Function Methods with Density Functional Theory for Excited States. *Chem. Rev.* **2018**, *118*, 7249–7292.

3. Becke, A. D. A New Mixing of Hartree-Fock and Local Density Functional Theories. *J. Chem. Phys.* **1993**, *98*, 1372-1377.

4. Becke, A. D. Density-Functional Thermochemistry. III. The Role of Exact Exchange. *J. Chem. Phys.* **1993**, *98*, 5648-5653.

5. Peverati, R.; Truhlar, D. G. Quest for a Universal Density Functional: The Accuracy of Density Functionals Across a Broad Spectrum of Databases in Chemistry and Physics. *Philos. Trans. R. Soc. London, Ser. A* **2014**, *372*, 20120476.

6. Seidl, A.; Görling, A.; Vogl, P.; Majewski, J. A.; Levy, M. Generalized Kohn-Sham Schemes and the Band-Gap Problem. Phys. Rev. B 1996, 53, 3764-3774.

7. Maier, T. M.; Arbuznikov, A. V.; Kaupp, M. Local Hybrid Functionals: Theory, Implementation, and Performance of an Emerging New Tool In Quantum Chemistry and Beyond. *Wiley Interdisc. Rev. Comput. Mol. Sci.* **2019,** *9*, e1378.

8. Peverati, R.; Truhlar, D. G. Improving the Accuracy of Hybrid Meta-GGA Density Functionals by Range Separation. *J. Phys. Chem. Lett.* **2011**, *2*, 2810–2817.

9. Zhao, Y.; Lynch, B. J.; Truhlar, D. G. Development and Assessment of a New Hybrid Density Functional Method for Thermochemical Kinetics. *Phys. Chem. Chem. Phys.* **2004**, *6*, 673-676.

10. Zhao, Y.; Truhlar, D. G. Hybrid Meta Density Functional Theory Methods for Thermochemistry, Thermochemical Kinetics, and Noncovalent Interactions: The MPW1B95 and MPWB1K Models and Comparative Assessments for Hydrogen Bonding and van der Waals Interactions. *J. Phys. Chem. A* **2004**, *108*, 6908-6918.

11. Zhao, Y.; Truhlar, D. G. Benchmark Databases for Nonbonded Interactions and Their Use to Test Density Functional Theory. *J. Chem. Theory Comput.* **2005**, *1*, 415–432.

12. Zhao, Y.; Truhlar, D. G. Design of Density Functionals that are Broadly Accurate for Thermochemistry, Thermochemical Kinetics, and Nonbonded Interactions. *J. Phys. Chem. A* **2005**, *109*, 5656–5667.

13. Zhao, Y.; Truhlar, D. G. The M06 Suite of Density Functionals for Main Group Thermochemistry, Thermochemical Kinetics, Noncovalent Interactions, Excited States, and Transition Elements: Two New Functionals and Systematic Testing of Four M06-Class Functionals and 12 Other Functionals. *Theor. Chem. Acc.* **2008**, *120*, 215–241.

14. Yu, H. S.; Zhang, W.; Verma, P.; He, X.; Truhlar, D. G. Nonseparable Exchange–Correlation Functional for Molecules, Including Homogeneous Catalysis Involving Transition Metals. *Phys. Chem. Chem. Phys.* **2015**, *17*, 12146-12160.

15. Yu, H. S.; He, X.; Truhlar, D. G. MN15-L: A New Local Exchange-Correlation Functional for Kohn–Sham Density Functional Theory with Broad Accuracy for Atoms, Molecules, and Solids. *J. Chem. Theory Comput.* **2016**, *12*, 1280-1293.

16. Yu, H. S.; He, X.; Li, S. L.; Truhlar, D. G. MN15: A Kohn–Sham Global-Hybrid Exchange–Correlation Density Functional with Broad Accuracy for Multi-Reference and Single-Reference Systems and Noncovalent Interactions. *Chem. Sci.* **2016**, *7*, 5032-5051.

17. Wang, Y.; Jin, X. S.; Yu, H. S.; Truhlar, D. G.; He, X. Revised M06-L Functional for Improved Accuracy on Chemical Reaction Barrier Heights, Noncovalent Interactions, and Solid-State Physics. *Proc. Natl. Acad. Sci. USA* **2017**, *114*, 8487-8492.

18. Wang, Y.; Verma, P.; Jin, X. S.; Truhlar, D. G.; He, X. Revised M06 Density Functional for Main-Group and Transition-Metal Chemistry. *Proc. Natl. Acad. Sci. USA* **2018**, *115*, 10257-10262.

19. Goerigk, L.; Hansen, A.; Bauer, C.; Ehrlich, S.; Najibi, A.; Grimme, S. A Look at the Density Functional Theory Zoo with the Advanced GMTKN55 Database for General Main Group Thermochemistry, Kinetics and Noncovalent Interactions. *Phys. Chem. Chem. Phys.* **2017**, *19*, 32184-32215.

20. Schultz, N. E.; Zhao, Y.; Truhlar, D. G. Density Functionals for Inorganometallic and Organometallic Chemistry. *J. Phys. Chem. A* **2005**, *109*, 11127–11143.

21. Yu, H. S.; Truhlar, D. G. Components of the Bond Energy in Polar Diatomic Molecules, Radicals, and Ions Formed by Group-1 and Group-2 Metal Atoms. *J. Chem. Theory Comput.* **2015**, *11*, 2968-2983.

22. Zhang, W.; Truhlar, D. G.; Tang, M. Tests of Exchange-Correlation Functional Approximations Against Reliable Experimental Data for Average Bond Energies of 3d Transition Metal Compounds. *J. Chem. Theory Comput.* **2013**, *9*, 3965-3977.

23. Lynch, B. J.; Truhlar, D. G. Small Representative Benchmarks for Thermochemical Calculations. *J. Phys. Chem. A* **2003**, *107*, 8996–8999.

24. Averkiev, B. B.; Zhao, Y.; Truhlar, D. G. Binding Energy of d^{10} Transition Metals to Alkenes by Wave Function Theory and Density Functional Theory. *J. Mol. Catal. A* **2010**, *324*, 80–88.

25. Xu, X.; Zhang, W.; Tang, M.; Truhlar, D. G. Do Practical Standard Coupled Cluster Calculations Agree Better than Kohn-Sham Calculations with Currently Available Functionals when Compared to the Best Available Experimental Data for Dissociation Energies of Bonds to 3d Transition Metals? *J. Chem. Theory Comput.* **2015**, *11*, 2036-2052.

26. Hoyer, C. E.; Manni, G. L.; Truhlar, D. G.; Gagliardi, L. Controversial Electronic Structures and Energies of Fe_2, Fe_2^+, and Fe_2^- Resolved by RASPT2 Calculations. *J. Chem. Phys.* **2014**, *141*, 204309-204309.

27. Zheng, J.; Zhao, Y.; Truhlar, D. G. The DBH24/08 Database and its Use to Assess Electronic Structure Model Chemistries for Chemical Reaction Barrier Heights. *J. Chem. Theory Comput*. **2009**, *5*, 808–821.

28. Lynch, B. J.; Truhlar, D. G. What Are the Best Affordable Multi-Coefficient Strategies for Calculating Transition State Geometries and Barrier Heights? *J. Phys. Chem. A* **2002**, *106*, 842–846.

29. Marshall, M. S.; Burns, L. A.; Sherrill, C. D. Basis Set Convergence of the Coupled-Cluster Correction, δ(MP2)(CCSD(T)): Best Practices for Benchmarking Non-Covalent Interactions and the Attendant Revision of the S22, NBC10, HBC6, and HSG Databases. *J. Chem. Phys.* **2011**, *135*, 194102.

30. McMahon, J. D.; Lane, J. R. Explicit Correlation and Basis Set Superposition Error: The Structure and Energy of Carbon Dioxide Dimer. *J. Chem. Phys.* **2011**, *135*, 2836-2843.

31. de Lange, K. M.; Lane, J. R. Explicit Correlation and Intermolecular Interactions: Investigating Carbon Dioxide Complexes with the CCSD(T)-F12 Method. *J. Chem. Phys.* **2011**, *134*, 123-127.

32. Vydrov, O. A.; Van Voorhis, T. Benchmark Assessment of the Accuracy of Several van der Waals Density Functionals. *J. Chem. Theory Comput*. **2012**, *8*, 1929-1934.

33. Tang, K. T.; Toennies, J. P. The van der Waals Potentials Between All the Rare Gas Atoms from He to Rn. *J. Chem. Phys.* **2003**, *118*, 4976-4983.

34. Řezáč, J.; Riley, K. E.; Hobza, P. S66: A Well-Balanced Database of Benchmark Interaction Energies Relevant to Biomolecular Structures. *J. Chem. Theory Comput*. **2011**, *7*, 2427-2438.

35. Peverati, R.; Truhlar, D. G. An Improved and Broadly Accurate Local Approximation to the Exchange–Correlation Density Functional: The MN12-L Functional for Electronic Structure Calculations in Chemistry and Physics. *Phys. Chem. Chem. Phys*. **2012**, *14*, 13171–13174.

36. Luo, S.; Averkiev, B. B.; Yang, K. R.; Xu, X.; Truhlar, D. G. Density Functional Theory of Open-Shell Systems. The 3d-Series Transition-Metal Atoms and Their Cations. *J. Chem. Theory Comput*. **2014**, *10*, 102-121.

37. Zhao, Y.; Truhlar, D. G. Assessment of Density Functionals for Pi Systems: Energy Differences Between Cumulenes and Poly-ynes and Proton Affinities, Bond Length Alternation, and Torsional Potentials of Conjugated Polyenes, and Proton Affinities of Conjugated Schiff Bases. *J. Phys. Chem. A* **2006**, *110*, 10478-10486.

38. Schwabe, T. An Isomeric Reaction Benchmark Set to Test if the Performance of State-of-the-Art Density Functionals Can be Regarded as Independent of the External Potential. *Phys. Chem. Chem. Phys.* **2014**, *16*, 14559-14567.

39. Luo, S.; Zhao, Y.; Truhlar, D. G. Validation of Electronic Structure Methods for Isomerization Reactions of Large Organic Molecules. *Phys. Chem. Chem. Phys.* **2011**, *13*, 13683-13689.

40. Zhao, Y.; Schultz, N. E.; Truhlar, D. G. Exchange-Correlation Functional with Broad Accuracy for Metallic and Nonmetallic Compounds, Kinetics, and Noncovalent Interactions, *J. Chem. Phys.* **2005**, *123*, 161103.

41. Zhao, Y.; Truhlar, D. G. A New Local Density Functional for Main Group Thermochemistry, Transition Metal Bonding, Thermochemical Kinetics, and Noncovalent Interaction. *J. Chem. Phys.* **2006**, *125*, 194101.

42. Chakravorty, S.; Gwaltney, S.; Davidson, E. R.; Parpia, F.; Fischer, C. Ground-State Correlation Energies for Atomic Ions with 3 to 18 Electrons. *Phys. Rev. A* **1993**, *47*, 3649-3670.

43. Peverati, R.; Zhao, Y.; Truhlar, D. G. Generalized Gradient Approximation that Recovers the Second-Order Density-Gradient Expansion with Optimized Across-the-Board Performance. *J. Phys. Chem. Lett.* **2011**, *2*, 1991-1997.

44. NIST WebBook, http://webbook.nist.gov/cgi/cbook.cgi?ID=C7664939&Units=SI&Mask=1#Thermo-Gas, accessed on July 26, 2015.

45. NIST WebBook, http://webbook.nist.gov/cgi/cbook.cgi?ID=C63344865&Units=SI, accessed on July 26, 2015.

46. NIST WebBook, http://webbook.nist.gov/cgi/cbook.cgi?ID=C7446119&Units=SI, accessed on July 26, 2015.

47. Peverati, R.; Truhlar, D. G. Exchange–Correlation Functional with Good Accuracy for Both Structural and Energetic Properties While Depending Only on the Density and its Gradient. *J. Chem. Theory Comput.* **2012**, *8*, 2310-2319.

48. Posada-Borbón, A.; Posada-Amarillas, A. Theoretical DFT Study of Homonuclear and Binary Transition-Metal Dimers. *Chem. Phys. Lett.* **2014**, *618*, 66–71.

49. NIST Compuational Chemistry Comparison and Benchmark Database: Experimental Bond Lengths (http://cccbdb.nist.gov/expbondlengths1.asp, accessed on Oct. 29, 2014.

50. Luo, S.; Truhlar, D. G. How Evenly Can Approximate Density Functionals Treat the Different Multiplicities and Ionization States of 4d Transition Metal Atoms? *J. Chem. Theory Comput.* **2012**, *8*, 4112-4126.

51. Yang, K.; Peverati, R.; Truhlar, D. G.; Valero, R. Density Functional Study of Multiplicity-Changing Valence and Rydberg Excitations of p-Block Elements: Delta Self-Consistent Field, Collinear Spin-Flip Time-Dependent Density Functional Theory (DFT), and Conventional Time-Dependent DFT. *J. Chem. Phys.* **2011**, *135*, 044118.

52. Isegawa, M.; Truhlar, D. G. Valence Excitation Energies of Alkenes, Carbonyl Compounds, and Azabenzenes by Time-Dependent Density Functional Theory: Linear Response of the Ground State Compared to Collinear and Noncollinear Spin-Flip TDDFT with the Tamm-Dancoff Approximation. *J. Chem. Phys.* **2013**, *138*, 134111.

53. Stein, T.; Kronik, L.; Baer, R. Reliable Prediction of Charge Transfer Excitations in Molecular Complexes Using Time-Dependent Density Functional Theory. *J. Am. Chem. Soc.* **2009**, *131*, 2818–2820.

54. Schreiber, M.; Silva-Junior, M. R.; Sauer, S. P. A; Thiel, W. Benchmarks for Electronically Excited States: CASPT2, CC2, CCSD, and CC3. *J. Chem. Phys.* **2008**, *128*, 134110.

55. Hoyer, C. E.; Ghosh, S.; Truhlar, D. G.; Gagliardi, L. Multiconfiguration Pair-Density Functional Theory Is as Accurate as CASPT2 for Electronic Excitation. *J. Phys. Chem. Lett.* **2016**, *7*, 586–591.

56. Verma, P.; Truhlar, D. G. HLE16: A Local Kohn–Sham Gradient Approximation with Good Performance for Semiconductor Band Gaps and Molecular Excitation Energies. *J. Phys. Chem. Lett.* **2017**, *8*, 380–387.

57. Ghosh, S.; Sonnenberger, A, L.; Hoyer, C, E.; Truhlar, D, G.; Gagliardi, L. Multiconfiguration Pair-Density Functional Theory Outperforms Kohn–Sham Density Functional Theory and Multireference Perturbation Theory for Ground-State and Excited-State Charge Transfer. *J. Chem. Theory Comput.* **2015**, *11*, 3643–3649.

58. Zhao, Y.; Ng, H. T.; Peverati, R.; Truhlar, D. G. Benchmark Database for Ylidic Bond Dissociation Energies and its Use for Assessments of Electronic Structure Methods. *J. Chem. Theory Comput.* **2012**, *8*, 2824–2834.

59. Hu, L.; Chen, H. Assessment of DFT Methods for Computing Activation Energies of Mo/W-Mediated Reactions. *J. Chem. Theory Comput.* **2015**, *11*, 4601-4614.

60. Sun, Y.; Chen, H. Performance of Density Functionals for Activation Energies of Zr-Mediated Reactions. *J. Chem. Theory Comput.* **2013**, *9*, 4735-4743.

61. Sun, Y.; Chen, H. Performance of Density Functionals for Activation Energies of Re-Catalyzed Organic Reactions. *J. Chem. Theory Comput.* **2014**, *10*, 579–588.

62. Weymuth, T.; Couzijn, E. P.; Chen, P.; Reiher, M. New Benchmark Set of Transition-Metal Coordination Reactions for the Assessment of Density Functionals. *J. Chem. Theory Comput.* **2014**, *10*, 3092-3103.

63. Husch, T.; Freitag, L.; Reiher, M. Calculation of Ligand Dissociation Energies in Large Transition-Metal Complexes. *J. Chem. Theory Comput.* **2018**, *14*, 2456-2468.

64. Leverentz, H. R.; Siepmann, J. I.; Truhlar, D. G.; Loukonen, V.; Vehkamäki, H. Energetics of Atmospherically Implicated Clusters Made of Sulfuric Acid, Ammonia, and Dimethyl Amine. *J. Phys. Chem. A* **2013**, *117*, 3819–3825.

65. Marenich, A. V.; Jerome, S. V.; Cramer, C. J.; Truhlar, D. G. Charge Model 5: An Extension of Hirshfeld Population Analysis for the Accurate Description of Molecular Interactions in Gaseous and Condensed Phases. *J. Chem. Theor. Comput.* **2012**, *8*, 527– 541.

66. Verma, P.; Truhlar, D. G. Can Kohn–Sham Density Functional Theory Predict Accurate Charge Distributions for Both Single-Reference and Multi-Reference Molecules? *Phys. Chem. Chem. Phys.* **2017**, *19*, 12898-12912.

67. Tang, K. T.; Toennies, J. P. The van der Waals Potentials Between All the Rare Gas Atoms from He to Rn. *J. Chem. Phys.* **2003**, *118*, 4976–4983.

68. Xu, X.; Alecu, I. M.; Truhlar, D. G. How Well Can Modern Density Functionals Predict Internuclear Distances at Transition States? *J. Chem. Theory Comput.* **2011**, *7*, 1667-1676.

69. Piccardo, M.; Penocchio, E.; Puzzarini, C.; Biczysko, M.; Barone, V. Semi-Experimental Equilibrium Structure Determinations by Employing B3LYP/SNSD Anharmonic Force Fields: Validation and Application to Semirigid Organic Molecules. *J. Phys. Chem. A* **2015**, *119*, 2058–2082.

70. Posada-Borbón, A.; Posada-Amarillas, A. Theoretical DFT Study of Homonuclear and Binary Transition-Metal Dimers. *Chem. Phys. Lett.* **2014**, *618*, 66–71.

71. Hoyer, C. E.; Gagliardi, L.; Truhlar, D. G. Multiconfiguration Pair-Density Functional Theory Spectral Calculations Are Stable to Adding Diffuse Basis Functions. *J. Phys. Chem. Lett.* **2015**, *6*, 4184–4188.

72. Send, R.; Kühn, M.; Furche, F. Assessing Excited State Methods by Adiabatic Excitation Energies. *J. Chem. Theory Comput.* **2011**, *7*, 2376-2386.

73. Isegawa, M.; Peverati, R.; Truhlar, D. G. Performance of Recent and High-Performance Approximate Density Functionals for Time-Dependent Density Functional Theory Calculations of Valence and Rydberg Electronic Transition Energies. *J. Chem. Phys.* **2012**, *137*, 244104.

74. Zaari, R. R.; Wong, Y. Y. Photoexcitation of 11-*Z-cis*-7,8-dihydro retinal and 11-*Z-cis*-retinal: A Comparative Computational Study. *Chem. Phys. Lett.* **2009**, *469*, 224.

75. Li, R.; Zheng, J.; Truhlar, D. G. Density Functional Approximations for Charge Transfer Excitations with Intermediate Spatial Overlap. *Phys. Chem. Chem. Phys.* **2010**, *12*, 12697–12701.

76. Weigend, F.; Ahlrichs, R. Balanced Basis Set of Split Valence, Triple Zeta and Quadruple Zeta Valence Quality for H to Rn: Design and Assessment of Accuracy. *Phys. Chem. Chem. Phys*. **2005**, *7*, 3297–3305.

77. Dunning, Jr., T. H. Gaussian Basis Sets for Use in Correlated Molecular Calculations. I. The Atoms Boron Through Neon and Hydrogen. *J. Chem. Phys.* **1989**, *90*, 1007–1023.

78. Dunning, Jr., T. H.; Peterson, K. A.; Wilson, A. K. Gaussian Basis Sets for Use in Correlated Molecular Calculations. X. The Atoms Aluminum Through Argon Revisited. *J. Chem. Phys*. **2001**, *114*, 9244–9253.

79. Papajak, E.; Truhlar, D. G. Convergent Partially Augmented Bases for Post-Hartree-Fock Calculations of Molecular Properties and Reaction Barrier Heights. *J. Chem. Theory Comput.* **2011***, 7*, 10–18.

80. Lynch, B. J.; Zhao, Y.; Truhlar, D. G. Effectiveness of Diffuse Basis Functions for Calculating Relative Energies by Density Functional Theory. *J. Phys. Chem. A* **2003**, *107*, 1384–1388.

81. Zhao, Y.; Truhlar, D. G. Exploring the Limit of Accuracy of the Global Hybrid Meta Density Functional for Main-Group Thermochemistry, Kinetics, and Noncovalent Interactions. *J. Chem. Theory Comput.* **2007**, *4*, 1849–1868.

82. Peterson, K. A.; Figgen, D.; Dolg, M.; Stoll, H. Energy-Consistent Relativistic Pseudopotentials and Correlation Consistent Basis Sets for the 4*d* elements Y–Pd. *J. Chem. Phys.* **2007**, *126*, 124101.

83. Martin, J. M. L.; Sundermann, A. Correlation Consistent Valence Basis Sets for Use with the Stuttgart–Dresden–Bonn Relativistic Effective Core Potentials: The atoms Ga–Kr and In–Xe. *J. Chem. Phys.* **2001**, *114*, 3408.

84. Krishnan, R.; Binkley, J. S.; Seeger, R.; Pople, J. A. Self-Consistent Molecular Orbital Methods. 20. Basis Set for Correlated Wave-Functions. *J. Chem. Phys*. **1980**, *72*, 650–654.

85. Amin, E. A.; Truhlar, D. G. Zn Coordination Chemistry: Development of Benchmark Suites for Geometries, Dipole Moments and Bond Dissociation Energies and Their Use to Test and Validate Density Functionals and Molecular Orbital Theory. *J. Chem. Theory Comput*. **2008**, *4*, 75–85.

86. Woon, D. E.; Dunning, Jr., T. H. Gaussian Basis Sets for Use in Correlated Molecular Calculations. III. The Second Row Atoms, Al–Ar. *J. Chem. Phys.* **1993**, *98*, 1358–1371.

87. Kendall, R. A.; Dunning, Jr., T. H.; Harrison, R. J. Electron Affinities of the First-Row Atoms Revisited. Systematic Basis Sets and Wave Functions. *J. Chem. Phys.* **1992**, *96*, 6796–6806.

88. Wilson, A. K.; Woon, D. E.; Peterson, K. A.; Dunning, Jr., T. H. Gaussian Basis Sets for Use in Correlated Molecular Calculations. IX. The Atoms Gallium Through Krypton. *J. Chem. Phys.***1999**, *110*, 7667–7676.

89. Prascher, B. P.; Woon, D. E.; Peterson, K. A.; Dunning, Jr., T. H.; Wilson, A. K. Gaussian Basis Sets for Use in Correlated Molecular Calculations. VII. Valence and Core-Valence Basis Sets for Li, Na, Be, and Mg. *Theor. Chem. Acc.* **2011**, *128*, 69–82.

90. Peterson, K. A.; Puzzarini, C. Systematically Convergent Basis Sets for Transition Metals. II. Pseudopotential-Based Correlation Consistent Basis Sets for the Group 11 (Cu, Ag, Au) and 12 (Zn, Cd, Hg) Elements. *Theor. Chem. Acc.* **2005**, *114*, 283–296.

91. Zheng, J.; Xu, X.; Truhlar, D. G. Minimally Augmented Karlsruhe Basis Sets. *Theor. Chem. Acc*. **2011**, *128*, 295–305.

92. Hehre, W. J.; Ditchfield, R.; Pople, J. A. Self-Consistent Molecular Orbital Methods. XII. Further Extensions of Gaussian-Type Basis Sets for Use in Molecular Orbital Studies of Organic Molecules. *J. Chem. Phys*. **1972**, *56*, 2257.

93. Wiberg, K. B.; de Oliveira, A. E.; Trucks, G. A Comparison of the Electronic Transition Energies for Ethene, Isobutene, Formaldehyde, and Acetone Calculated Using RPA, TDDFT, and EOM-CCSD. Effect of Basis Sets. *J. Phys. Chem. A* **2002**, *106*, 4192–4199.

94. Frisch, M. J.; Trucks, G. W.; Schlegel, H. B.; Scuseria, G. E.; Robb, M. A.; Cheeseman, J. R.; Scalmani, G.; Barone, V.; Mennucci, B.; Petersson, G. A.; et al. *Gaussian 09*, Revision C.01, Gaussian, Inc.: Wallingford CT, 2010.

95. Frisch, M. J.; Trucks, G. W.; Schlegel, H. B.; Scuseria, G. E.; Robb, M. A.; Cheeseman, J. R.; Scalmani, G.; Barone, V.; Petersson, G. A.; Nakatsuji, H.; et al. *Gaussian 16*, Revision A.03, Gaussian, Inc.: Wallingford CT, 2016.

96. Zhao, Y.; Peverati, R.; Yang, K. R.; Luo, S.; Yu, H. S.; He, X.; Wang, Y.; Verma, P.; Truhlar, D. G. *MN-GFM*, version 6.10: Minnesota–Gaussian Functional Module. http://comp.chem.umn.edu/mn-gfm (accessed Aug. 10, 2018).

97. Hess, B. A. Relativistic Electronic-Structure Calculations Employing a 2-Component No-Pair Formalism with External-Field Projection Operators. *Phys. Rev. A* **1986**, *33*, 3742–3748.

98. Krukau, A. V.; Vydrov, O. A.; Izmaylov, A. F.; Scuseria, G. E. Influence of the Exchange Screening Parameter on the Performance of Screened Hybrid Functionals. *J. Chem. Phys.* **2006**, *125*, 224106.

99. Henderson, T. M.; Izmaylov, A. F.; Scalmani, G.; Scuseria, G. E. Can Short-Range Hybrids Describe Long-Range-Dependent Properties? *J. Chem. Phys.* **2009**, *131*, 044108.

100. Peverati, R.; Truhlar, D. G. Screened-Exchange Density Functionals with Broad Accuracy for Chemistry and Solid-State Physics. *Phys. Chem. Chem. Phys*. **2012**, *14*, 16187–16191.

101. Henderson, T. M.; Izmaylov, A. F.; Scuseria, G. E.; Savin, A. The Importance of Middle-Range Hartree-Fock-Type Exchange for Hybrid Density Functionals. *J. Chem. Phys.* **2007**, *127*, 221103.

102. Henderson, T. M.; Izmaylov, A. F.; Scuseria, G. E.; Savin, A. Assessment of a Middle Range Hybrid Functional. *J. Chem. Theory Comput.* **2008**, *4*, 1254.

103. Vydrov, O. A.; Scuseria, G. E. Assessment of a Long-Range Corrected Hybrid Functional. *J. Chem. Phys.* **2006**, *125*, 234109.

104. Chai, J.-D.; Head-Gordon, M. Systematic Optimization of Long-Range Corrected Hybrid Density Functionals. *J. Chem. Phys.* **2008**, *128*, 084106.

105. Chai, J.-D.; Head-Gordon, M. Long-Range Corrected Hybrid Density Functionals with Damped Atom–Atom Dispersion Corrections. *Phys. Chem. Chem. Phys.* **2008**, *10*, 6615-6620.

106. Yanai, T.; Tew, D. P.; Handy, N. C. A New Hybrid Exchange–Correlation Functional Using the Coulomb-Attenuating Method (CAM-B3LYP). *Chem. Phys. Lett.* **2004**, *393*, 51–57.

107. Perdew, J. P.; Burke, K.; Ernzerhof, M. Generalized Gradient Approximation Made Simple. *Phys. Rev. Lett.* **1996**, *77*, 3865-3868.

108. Becke, A. D. Density-Functional Exchange-Energy Approximation with Correct Asymptotic Behavior. *Phys. Rev. A* **1988**, *38*, 3098-3100.

109. Lee, C.; Yang, W.; Parr, R. G. Development of the Colle-Salvetti Correlation-Energy Formula into a Functional of the Electron Density. *Phys. Rev. B* **1988**, *37*, 785-789.

110. Tao, J.; Perdew, J. P.; Staroverov, V. N.; Scuseria, G. E. Climbing the Density Functional Ladder: Nonempirical Meta-Generalized Gradient Approximation Designed for Molecules and Solids. *Phys. Rev. Lett.* **2003**, *91*, 146401.

111. Stephens, P. J.; Devlin, F. J.; Chabalowski, C. F.; Frisch, M. J. Ab Initio Calculation of Vibrational Absorption and Circular Dichroism Spectra Using Density Functional Force Fields. *J. Phys. Chem.* **1994**, *98*, 11623–11627.

112. Adamo, C.; Barone, V. Toward Reliable Density Functional Methods Without Adjustable Parameters: The PBE0 Model. *J. Chem. Phys.* **1999**, *110*, 6158–6170.

113. Yu, H. S.; Zhao, Y.; Peverati, R.; He, X.; Wang, Y.; Verma, P.; Truhlar, D. G. Minnesota Functional Module, version 4.0; University of Minnesota: Minneapolis, 2018; https://comp.chem.umn.edu/mfm (accessed Dec. 1, 2018)

114. Peach, M. J. G.; Le Sueur, C. R.; Ruud, K.; Guillaume, M.; Tozer, D. J. TDDFT Diagnostic Testing and Functional Assessment for Triazene Chromophores. *Phys. Chem. Chem. Phys.* **2009**, *11*, 4465-4470.

115. Livshits, E.; Baer, R. A Well-Tempered Density Functional Theory of Electrons in Molecules. *Phys. Chem. Chem. Phys.* **2007**, *9*, 2932–2941.

116. Bao, J. L.; Verma, P.; Truhlar, D. G. How Well Can Density Functional Theory and Pair-Density Functional Theory Predict the Correct Atomic Charges for Dissociation and Accurate Dissociation Energetics of Ionic Bonds? *Phys. Chem. Chem. Phys.* **2018**, *20*, 23072–23078.

117. Li, S. L.; Truhlar, D. G. Improving Rydberg Excitations Within Time-Dependent Density Functional Theory with Generalized Gradient Approximations: The Exchange-Enhancement-for-Large-Gradient Scheme. *J. Chem. Theory Comput.* **2015**, *11*, 3123-3130.

118. Li Manni, G.; Carlson, R. K.; Luo, S.; Ma, D.; Olsen, J.; Truhlar, D. G.; Gagliardi, L. Multiconfiguration Pair-Density Functional Theory. *J. Chem. Theory Comput.* **2014**, *10*, 3669−3680.

119. Verma, P.; Truhlar, D. G. HLE17: An Improved Local Exchange-Correlation Functional for Computing Semiconductor Band Gaps and Molecular Excitation Energies. *J. Phys. Chem. C* **2017***, 121*, 7144−7154.

120. Janesko, B. G. Rung 3.5 Density Functionals. *J. Chem. Phys.* **2010**, *133*, 104103.

121. Janesko, B. G.; Proynov, E.; Scalmani, G.; Frisch, M. J. Long-Range-Corrected Rung 3.5 Density Functional Approximations. *J. Chem. Phys.* **2018**, *148*, 104112.

TOC graphic:

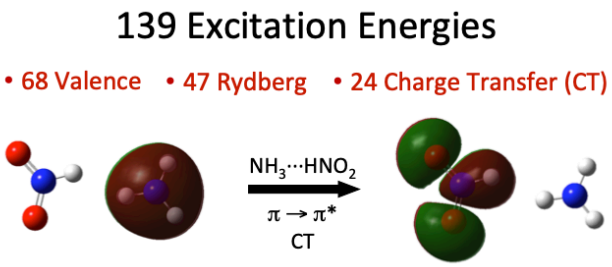

eV	revM11	M11	LC-ωPBE
MUE (all 139)	0.35	0.49	0.42